Ricardo André Martins Pastilha Vieira

Licenciado em Ciências de Engenharia Biomédica

Polypyrrole functionalized electrospun fibers for electrically stimulated drug release

Dissertação para obtenção do Grau de Mestre em

Engenharia Biomédica

Orientadora: Ana Baptista, Investigadora, DCM-FCT/UNL

Co-orientadora: Isabel Ferreira, Professora Associada, DCM-FCT/UNL

FACULDADE DE CIÊNCIAS E TECNOLOGIA
UNIVERSIDADE NOVA DE LISBOA

Setembro, 2019

Polypyrrole functionalized electrospun fibers for electrically stimulated drug release

Este documento foi gerado utilizando o processador (pdf)LaTeX, com base no template "novathesis" [1] desenvolvido no Dep. Informática da FCT-NOVA [2].
[1] https://github.com/joaomlourenco/novathesis [2] http://www.di.fct.unl.pt

To everyone who joined me in this crazy adventure!

Acknowledgements

I would first like to thank my supervisors, Dr. Ana Baptista and Prof. Dr. Isabel Ferreira, for every advise, every help and all the learning experience I got from you. I would like to express my gratitude for your kindness and patience.

To all my lab friends, the new and the ones I had already met before, a toast to all the daily adventures we shared together! Thank you for helping me in every situation, for sharing with me the craziest thoughts and histories and for giving this scientist-life experience a whole new spirit!

To my great friend, Sofia Silvestre, tons of kisses for all the help you gave me throughout these 5 years and for the eternal friendship we built!

To my oldest friends, my big boys, a huge hug for being who you are, every time!

To my dear and beautiful girlfriend, Sara, I owe you the world and all the greatest things it has to offer! Thank you and thank you and thank you again for all your love, patience, kindness and happiness! I Love you with all my heart!

And last but not the least, a huge thanks to my amazing family! For sharing this spectacular ride that my life is on a daily basis! Lots of kisses, hugs and love to my papa, mama and my little big sister! Love you all as well!

This work was partially funded by H2020-ICT-2014-1, RIA, TransFlexTeg-645241; ERC-CoG-2014, CapTherPV, 647596; ERC-POC-2019, CAPSEL, 855018

Abstract

Current infection therapies often require oral and topical drug administration. Over the years, several studies have proven the lack of efficiency that characterizes these treatments.

This work is focused on the development of an innovative biocompatible drug support, obtained by electrospinning using a polymer (Cellulose Acetate) with a drug model (Rhodamine B), resulting on a nanofiber mat with the drug encapsulated. The encapsulation was tested in both conventional and coaxial setups. The optimized membranes were also functionalized with a conductive polymer (polypyrrole) to test electrical drug delivery activation. Drug release profiles performed with passive (diffusion) and active stimulation (electrical stimulus) were analyzed and compared.

The results obtained allowed to conclude that both types of membranes (conventionally or coaxially produced) were uniformly polymerized 45 minutes after the beginning of the polymerization process. Moreover, positive stimulus polarity proved to induce a higher response in terms of drug release. Additionally, different studies were also performed with the aim of obtaining a better control over the released amount and release instants, being therefore studied the sensibility of the membranes to a switchable-like profile. As a result, it could be concluded that the higher the applied voltage, the closer the obtained release profile was from an "on-off" pattern.

Keywords: electrospinning, coaxial electrospinning, drug delivery system, cellulose acetate, rhodamine b, polypyrrole

Resumo

As terapias de infeção atuais requerem geralmente administração oral e tópica de fármacos. Ao longo dos anos, vários estudos comprovaram a falta de eficácia que caracteriza estes tratamentos.

Assim, este trabalho tem como foco o desenvolvimento de um substrato biocompatível inovador, obtido por eletrofiação de um polímero (acetato de celulose) com um modelo de fármaco (Rodamina B), resultando numa matriz de nanofibras com o fármaco encapsulado. Ambas as configurações, convencional e coaxial, foram estudadas e otimizadas, e as membranas resultantes foram posteriormente funcionalizadas com um polímero condutor (polipirrol). A cinética de libertação do fármaco foi analisada e os métodos de administração passiva (difusão) e ativa (estímulo elétrico) foram realizados e comparados.

Os resultados obtidos permitiram concluir que ambos os tipos de membranas (produzidas por via convencional e coaxial) foram uniformemente polimerizadas 45 minutos após o início do processo de polimerização. Além disso, a polaridade positiva do estímulo induziu uma maior resposta em termos de libertação do medicamento. Adicionalmente, diferentes estudos foram também realizados com o objetivo de obter um melhor controlo sobre a quantidade libertada, bem como sobre os instantes de libertação, sendo, por isso, estudada a sensibilidade das membranas a um perfil do tipo comutável. Como resultado, concluiu-se que, quanto maior a tensão aplicada, mais próximo de um padrão "on-off"o perfil de libertação obtido fica.

Palavras-chave: eletrofiação, eletrofiação coaxial, sistema de libertação de fármaco, acetato de celulose, rodamina b, polipirrol

Contents

List of Figures

List of Tables

Acronyms

BSA	Bovine Serum Albumin.
CA	Cellulose Acetate.
cm	Centimeter.
DMAc	Dimethylacetamid.
ES	Electrospinning.
g	Grams.
HFP	1,1,1,3,3,3-Hexafluoro-2-propanol.
I-V	Current-Voltage Characteristic Curve.
M	Molar.
mL	Millilitre.
mM	miliMolar.
NMA	Hydroxymethyl Acrylamide.
OM	Optical Microscopy.
PLGA	Poly (lactic-co-glycolic acid).
PLLA	Poly-L-Lactic Acid.

PLLACL	Poly(L-lactide-co-caprolactone.
PPy	Polypyrrole.
PVCL	Poly(vinyl caprolactam).
Py	Pyrrole.
RhB	Rhodamine B.
S	Siemens.
SEM	Scanning Electron Microscopy.
TEM	Transmission Electron Microscope.
V	Volts.

Chapter 1

Introduction

1.1 Motivation

The management of chronic wounds has emerged as a major health care challenge during the 21st century, consuming significant portions of healthcare budgets, in terms of the number of people affected and the expenses derived from their prevention and treatment [1]. Chronic wounds, where full regeneration of the damaged tissue does not complete in three months [2], such as diabetic foot ulcers, leg ulcers, or pressure sores have a significant negative impact on the quality of life of affected individuals. Smart systems that can monitor the wound environment without the need to visit so often the medical facilities are extremely beneficial and this was the onset for a new field of research, focusing mainly on sensors and actuators fabricated on flexible substrates.

Current infection therapies often require oral and topical antibiotic administration. However, this kind of methods need much larger dosage since a great part of the antibiotic gets wasted even before getting to the target location. Therefore, systems capable of delivering drugs via a more controlled way become more therapeutically efficient, induce less toxicity and decrease the number of doses administered [3].

Moreover, drug delivery systems are of particular importance as the ineffective vasculature in the wound bed can prevent effective delivery of drug to the healing tissue when the drug is administered systemically. In addition, the side effects of some drugs, the low half-life of biological factors, and the dynamicity of the wound environment require complex drug delivery systems that can deliver the active factors in proper dosage to the appropriate location [4].

In drug delivery systems, the encapsulated antibiotic can be released through different mechanisms which can be classified as active and passive delivery. In active delivery, the release is triggered in response to an environmental stimulus (pH, temperature, enzymes,

chemical reactions, redox reactions, etc.) or external stimuli (magnetic field, electric field, light, ultrasound, etc.) [4]. In contrast, passive delivery relies on the diffusion of the drug through the carrier matrix to reach the surrounding medium [5]. In this work, both kinds of mechanisms will be studied, being active delivery induced by an electrical stimulus and passive delivery studied for several conditions. An ideal application of an electrical stimulus would be one which allowed an overall control over the release method. Such control implies releasing the drug only if the stimulus had been applied and existing a direct relation between the stimulus duration/strength and the amount of drug release. This would give rise to an "on-off"release-like profile, in terms of the percentage of drug release over time. Compared to other types of drug release profiles, the one mentioned above would not only avoid the drug release burst, an excessive amount of drug that is released as soon as the membrane is immersed in solution, dangerously associated with high levels of toxicity, but also to an actuation on the wound area only at certain pre-defined moments, improving the treatment's efficacy.

Due to the limited regenerative capacity that characterizes the majority of the human tissues and with the aim of avoiding the injury and subsequent degeneration derived from such limitation, concepts like regenerative engineering emerged. Substrates capable of controlling drug release rate and regenerating injured tissues have been a main topic in research and development in this area. Among these, electrospun nanofibers offer unique features compared to other types of substrates, namely a large surface area-to-volume ratio, high porosity, uniformity in fiber size, flexibility and the ease of functionalization with several bioactive molecules [6]. Moreover, these devices are capable of embedding and deliver numerous drugs in a sustained and predictable way [7].

In this context, the work hereby presented aims to develop an innovative combination of a carrier-drug system, obtained via electrospinning technique, followed by its functionalization and finally the study of controlled drug release. By exploring new approaches to the topic of drug delivery using an innovative carrier-drug combination, the conclusions withdrawn from this work may help not only to contribute to a more economically sustainable solution of studying and developing these types of systems, but also to better understand how they work and how to optimize their efficiency.

1.2 State of the Art

The current work can be divided in three main tasks: membranes production, membranes functionalization and controlled drug release. Thereby, the following literature review will also be in accordance with these topics, being given detailed information about previous work performed in each of those three areas.

With respect to the nanofibers production, for both types of electrospinning setups (conventional and coaxial), the same carrier-drug system was used. As far as the author is concerned, it is the first time that this system is being studied, either in the aim of a drug release system, or in any other application. Therefore, this review will cover several

works within each topic, with a focus on the studies that worked with the same materials as the current one, however in a separate way. As the carrier, a Cellulose Acetate (CA) solution was chosen and, as the model drug, Rhodamine B was employed. Looking forward to obtain optimal work conditions, the preparation of such solutions needed to be carefully studied to optimize the work from such an early phase. Thereby, Tungprapa *et al*. 2007 [8] on their studies about the effect of solvent system on the morphology and fiber diameter concluded that one of the most versatile and consistent solvent system to perform CA electrospinning was the acetone:N,N-dimethylacetamide (DMAc) in the proportion of 2:1. Moreover, several attempts of blending CA with different drugs, namely Naproxen, Indomethacin, Ibuprofen, Sulindac and Curcumin, were performed using the same solvents proportion mentioned above [8], [9]. Supported by these evidences, this binary system was the solvent combination used in this work to prepare CA solutions.

Despite being introduced a few years before, only in 1934 had electrospinning been accepted as a nanofiber fabrication technique, with the work developed by Formhals [10],[11].

Since then, several authors published many works where they executed this technique under various conditions, in order to understand what parameters influenced the formation of a continuous and defect-free membrane. Enumerating only a few as an example, Taylor *et al*. 1969 [12] studied the effect of changes in the applied voltage; Zong and coworkers 2002 [13], in turn, found out that a minimum flow-rate of the polymer during the process is needed to replace the solution that is lost when the nanofiber jet is ejected; in a study conducted by Baumgarten 1971 [14], the relationship between distance to collector and size and morphology of the fibers was studied.

If the drug and the polymer are soluble in the same solvent, the drug can be dissolved directly into the polymer solution. Electrospinning of this kind of solutions results in the embedding of the drug in the nanofiber scaffold. However, in terms of drug release profile, an initial burst release is going to be expected, due to the drug distribution on the surface of the nanofibers, large nanofiber surface areas and the amorphous status of the drugs inside the nanofibers [15].

The burst release mentioned above continues to be one of the major weaknesses of drug release systems and is potentially harmful to patients in clinical applications. One possible solution to attenuate this effect would be to change nanofibers configuration in order to get a better drug encapsulation. With this purpose, in 2003, Sun *et al*. [16] introduced the concept of coaxial electrospinning. In their work, they obtained core-shell nanofibers made of two identical polymers (poly(ethylene oxide) and, in a similar way, they obtained a compound made of two different polymers (poly(ethylene oxide and poly(dodecylthiophene)). For the first time, a distinguishable separation between a shell and a core was obtained, as shown in Figure 1.1.

Such discovery brought numerous advantages to the field of drug release systems, among which a better encapsulation of the core material is one that motivated the use of co-electrospinning in this work, but it also requires some specific characteristics between

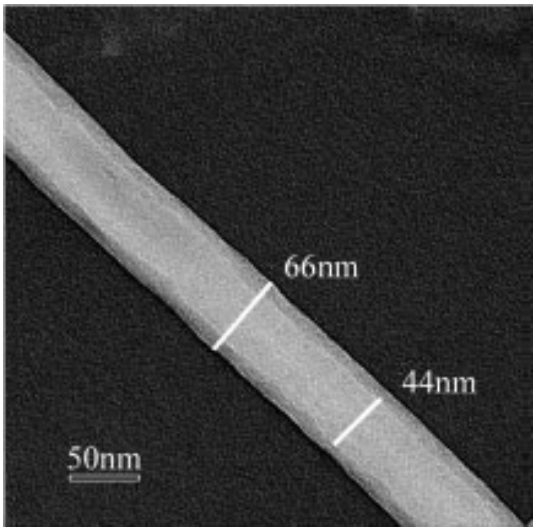

Figure 1.1: TEM of a compound nanofiber (adapted from [16]).

the materials involved. In terms of solution viscosities, co-electrospinning works better when the shell solution has a good spinnability and sufficient viscosity to overcome the interfacial tension between core and shell solutions [17].

Kao *et al.* 2015 [18] confirmed that, similar to the conventional electrospinning setup, the higher the concentration of the solutions, the higher the fibers diameter.

When choosing solution solvents, this process has to be made carefully so that a stable compound jet can be formed, with neither of them resulting in the precipitation of the other. Despite it has already been proven that two miscible solution can be electrospun [16], its tendency to get mixed up in the electrospinning process clearly overcomes the low probability of it to work correctly. Thereby, the ideal co-electrospinning is made of two immiscible solutions, since they ensure phase separation during the spinning process, as studied by Kurban *et al.* 2010 [19].

Moghe and Gupta 2008 [20] stated that for a given pair of polymer solutions, there is a small range of voltage values which can be applied so that a stable compound Taylor cone can be formed.

Identical to conventional electrospinning, in the coaxial process the flow rates chosen for both the core and the shell solution also have a crucial impact on the resulting fibers [17]. Interesting studies by Nguyen *et al.* 2012 [21] led to the conclusion that lower feed ratios resulted in higher stability of the core sheath structures, but at the same time, the inherent high viscous stress at these rate values resulted in the break down into several individual segments of the core material. According to Xia *et al.* 2014 [22], optimum flow rates combination is also related with the thickness of the resulting fibers.

Therefore, the first part of the work hereby presented will explore and combine these and other concepts that were mentioned above and apply it to the not yet explored combination of cellulose acetate-Rhodamine B system. A search for the optimal conditions to obtain nanofibers of the carrier-drug system chosen will be explained in the subsequent

chapters.

Once optimized and obtained the nanofibers mat, and since cellulose acetate fibers are characterized by a weak electrical conductivity [23], functionalization of these membranes with a conductive polymer is needed in order to turn them stimuli-responsive. Thereby, due to its high conductivity, biocompatibility and low-cost process [24], [25], Polypyrrole (PPy) was the polymer chosen to functionalize the membranes presented in this work.

Jin *et al.* 2016 [26] have successfully developed a conductive PPy-PLLA (poly-L-lactic acid) composite film, through casting film, to study an electrically controlled delivery system of the protein Bovine Serum Albumin (BSA). The electrical conductivity of PPy-PLLA composite film was $3.33 \pm 2.0 \times 10^{-3}$ S/cm.

More recently, Baptista and fellow research team [27] developed flexible, lightweight, non-toxic and conductive cellulose based electrospun fibers and functionalized them with PPy, by *in situ* polymerization. The approach done in the work here presented follows the same procedure as this one. In the mentioned study, a careful and detailed analysis was performed in terms of monomer concentrations, polymerization times and concentration of the oxidizing agent. Conductivity values increased remarkably up to 10^{-2} S/cm.

The first time electrospun fiber mats were studied as drug delivery vehicles, Kenawy *et al.* 2002 [28] used tetracycline hydrochloride as a model drug and the fibers were electrospun from chloroform solutions. Their work first introduced the concept of analyzing the drug release profile via UV-Vis spectroscopy.

That work was the onset for a major field of research and development nowadays. Up till now, many studies were driven by the aim of obtaining better and more efficient drug release systems.

Nista and coworkers [29] 2013 produced nanofiber membranes of cellulose acetate and tried out four different types of solvent combinations. Among the four detailed in their work, the one that most matters to reference here is the DMAc/acetone/water combination. The reason is related to the fact that in the presented work, the model drug will be dissolved in water and further electrospinned using the coaxial setup, where it will be in contact with cellulose acetate. The intended interaction between water and cellulose acetate is going to be tried out in order to get an optimal encapsulation of Rhodamine B, creating a barrier effect between the shell and the core of the nanofibers. Due to the incompatibility between water and cellulose acetate, understanding the proportion that must exist between both materials so that one does not lead to the precipitation of the other is important. In their work, Nista and her team used 63:32:5 ratio between the three solvents mentioned above, respectively.

In the study taken by Liao *et al.* 2009 [30], the hypothesis of impregnating a composite nanofiber mat (resultant of an emulsion which included poly (lactic-co-glycolic acid) (PLGA)) with Rhodamine B particles (used as a model compound to simulate drugs) was tested out, being studied its encapsulation/release performance. They concluded that the

composite nanofibers mat electrospun from the emulsion exhibited the desired controllable release performance. This study proved as a good example of how Rhodamine B can be used to model a drug in this kind of simulations.

González and Frey 2017 [31] worked on the development of stimuli-responsive nanofibers, in their case sensitive to temperature. Nanofibers were obtained from the conventional electrospinning of an innovative combination between Poly(vinyl caprolactam) (PVCL) and hydroxymethyl acrylamide (NMA), resulting in the formation of chemical hydrogel nanofibers. To study the sensitivity of nanofibers, Rhodamine B was incorporated by dissolving the dye directly in the initial electrospinning solution. As a result, they managed to analyze and built the release kinetics in function of an external stimulus.

The review, made so far, over the studies performed in the topic of drug release, covered just the conventional electrospinning technique. Looking to what has been done by taking advantage of the full potential that coaxial setup has to offer, several interesting works can also be found.

Entering in a dimension that overgoes the expectations of the present work, Su *et al.* 2012 [32] presented the scientific community a whole new set of capabilities that drug delivery systems have to offer. The purpose of their work was to develop a type of tissue-engineering scaffold with the capability of encapsulation and controlled release of dual drugs (Rhodamine B and Bovine Serum Albumin). Several combinations were tried, changing the location of both drugs (between the core and shell). Poly(L-lactide-co-caprolactone) (PLLACL) and 1,1,1,3,3,3-Hexafluoro-2-propanol (HFP) were the other fiber constituents, apart from the drugs. The main conclusions were that, from drug release profiles, it could be stated these are dependent on the location the drug or protein are put into. This can have significant implications depending on the type of application that will be given to these fibers, whether tissue regeneration, combined therapies or cancer treatments.

According to Giuseppi-Elie, in his review work [33], electro-stimulated drug release devices are devices that produce a programmed drug release profile influenced by the application of voltage or even current. To understand if the membranes produced and functionalized in this work are really sensitive to the electric stimulus, one of the objectives proposed is to study whether the carrier-drug system used is capable of showing a switch ON/OFF capability. This means that, by applying electrical stimulations, drug release should increase faster, decreasing its release speed during the periods of no application. The release profile of such drug delivery system would show a step-like curve throughout the graph. Studies developed by Pérez-Martinez *et al.* 2016 [34] and Li *et al.* 2015 [35], by using Rhodamine B as a model drug compound, succeed on their aim of getting this switch behavior. An example of an ON/OFF release profile is depicted in Figure 1.2.

Table 1.1 summarizes the most relevant research work presented above in each of the three parts this work is divided in.

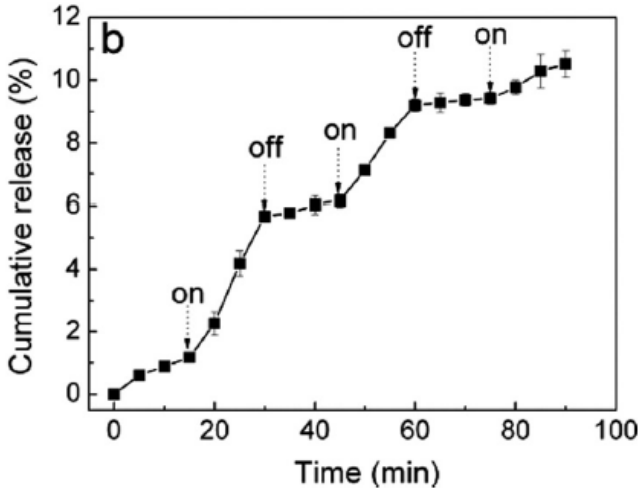

Figure 1.2: Release profile of Rhodamine B under an on-off voltage change (adapted from [35]).

Table 1.1: Overview of only the most relevant research made in each sub-category of the work structure.

DRUG DELIVERY SYSTEM					
MEMBRANES PRODUCTION		MEMBRANES FUNCTIONALIZATION		DRUG RELEASE TESTS	
Ref	Short Description	Ref	Short Description	Ref	Short Description
8	2:1 acetone:DMAc best combination	26	Conductive composite film. PPy was used and conductivity values measured	28	Pioneer work on this field of research
9, 10	Used same proportion to blend CA with 4 drugs	27	*In situ* optimal polymerization of PPy - will be used in this work	30	Combination between water and CA - without precipitating
12,13	Pioneering work in the electrospinning technique			30	RhB used as a compound to model a drug
14, 15, 16	Conventional ES parameters influence			31	Temperature stimuli-responsive nanofibers using RhB
18	Pioneer work in the development of a coaxial setup			32	Multiple-drug delivery
19-22	Parameters conditioning co-electrospinning			34,35	ON/OFF release profile

Chapter 2

Materials and Methods

In the following chapter, a detailed explanation of the materials and methods employed during the work will be given. Thereby, a look over the production of membranes process, its corresponding functionalization methods and several characterization techniques will be taken. Details about the performance of controlled release tests will also be explained.

2.1 Membranes Production

In this first section of the work here presented, the main goal was to use conventional and coaxial electrospinning parameters to produce polymer-based fibers with a model drug encapsulated. In both types of setups, cellulose acetate was used as the carrier polymer and Rhodamine B was chosen to model a drug.

- **Materials**
  - **Cellulose Acetate**

Due to its numerous applications, polymer fibers are the subject of several studies [36]. Although the industrial branch is the one that most benefits from such applications, an emerging interest in the study of these polymers for health applications has been noted. Particularly in the topics covered in this project, membrane production and drug-controlled release, the characteristics that are most sought in the polymers studied are their biocompatibility, cost-effectiveness relationship, toxicity and solubility.

In this context, one of the polymers that best matches the characteristics imposed is cellulose acetate. Being one of the most important organic esters derived from cellulose, Earth's major biopolymer, cellulose acetate results from the replacement of hydroxyl groups of each glucose unit by acetyl groups [37].

The mean number of hydroxyl groups replaced by acetyl groups express the degree of substitution [38]. This, in turn, is directly related to the crystallinity of the polymer, its biodegradability and solubility in different solvents, among other properties. Figure 2.1 shows the cellulose acetate structure. Given its advantageous features, namely its low cost, high level of biocompatibility and non-toxicity [39], [40], cellulose acetate was the polymer chosen to form the nanofibers studied in this work.

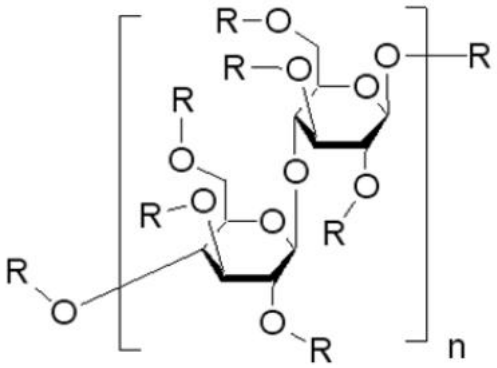

Figure 2.1: Cellulose Acetate Structure. R = CH_3CO or H (adapted from [41]).

– **Rhodamine B (RhB)**

Rhodamine B (Figure 2.2) is a synthetic organic dye, widely used as a fluorescent tracer in many applications due to its high water solubility, low cost and its corresponding emission spectra, which presents a distinguishable peak of absorption in the visible region [42]. These range of characteristics allows rhodamine B to be used, as reported several times, as a model drug with the aim of studying controlled-drug release systems.

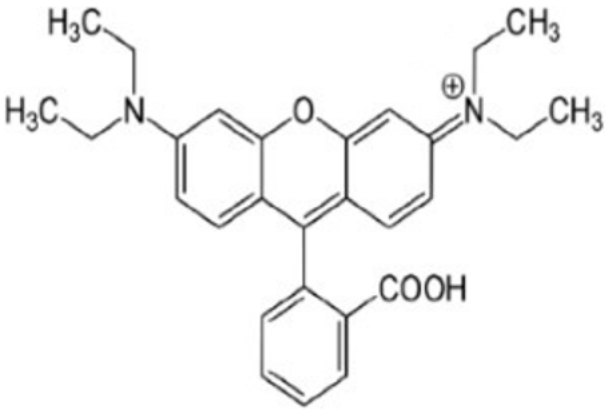

Figure 2.2: Rhodamine B Structure (adapted from [43]).

Its fluorescent magenta characteristic eases the process of absorbance readings, which in turn allows for a convenient representation of the amount released with respect to time. As previously stated in the Literature Review section, RhB has already been incorporated

in many studies using different electrospinning setups and in some cases followed by corresponding release study [31], [32], [35]. This helps to prove that RhB is not only a more economically-affordable solution to model a specific type of drug (one with similar chemical and molecular properties), but also to accurately mimic that kind of medication.

– **Solutions**

In terms of solutions preparation, in the case of conventional electrospinning, one solution was used, which consisted on a 8% (w/w) CA solution (Mn ~ 50000, 20-40% acetyl groups, Sigma-Aldrich) in 2:1 acetone:DMAc solvent mixture, to which were added 4.3 x 10^{-3} grams of Rhodamine B (≥ 95% (HPLC), Sigma-Aldrich), corresponding to the same mass weighted in the preparation of Rhodamine B solution used in coaxial setup. For coaxial electrospinning process, two solutions were prepared. The shell solution was the same CA solution with the same solvent mixture ratio detailed above, as for the core solution a 0.6 mM Rhodamine B was used. Apart from the detailed solutions above, few others were tried throughout the practical work, namely druing the coaxial electrospinning process. With the same solvent ratio mentioned before, a 12% (w/w) and a 18% (w/w) CA solutions were produced and tried out as shell solutions. For the core solution and in a similar preparation as the 0.6 mM solution, a 1.5 mM solution in the same water volume (20 mL) was developed and combined with different CA solutions.

- **Methods**

– **Electrospinning: conventional and coaxial setups**

Electrospinning is a widely used technology that utilizes the electric force to drive the spinning process and to produce polymer fibers. Diameters of the fibers produced can range from 2 nm to several micrometers, which differentiate electrospinning from other conventional techniques to produce fibers. The small size of each individual fiber leads, in turn, to large specific surface areas. This combined with the characteristic high porosity of the obtained fiber mat, with inter-connected porous network, allows for a better and easier encapsulation and immobilization of drug molecules. Additionally, the ability to modify surface properties of the obtained membranes, by means of functionalization processes, render electrospinning one of the most versatile fiber-fabrication techniques [30], [44], [45].

In a conventional electrospinning setup, a polymer solution is hosted in a syringe with a needle, to which a high voltage power supply is linked to, as depicted in Figure 2.3. When the voltage is applied, the particles within the solution are charged creating a repulsive force. At this point, the liquid drop that is on the tip of the needle is under several forces, namely the repulsive forces mentioned above, the attractive forces from the oppositely charged collector and the surface tension inherent to the polymer solution. As the electric field strength increases, electrostatic forces will also increase, until it reaches

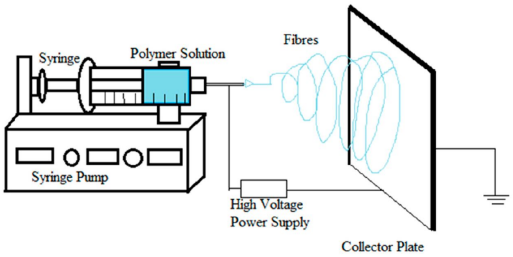

Figure 2.3: Conventional Electrospinning Setup (adapted from [46]).

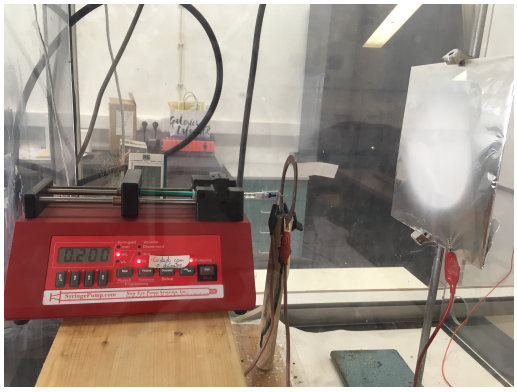

Figure 2.4: Conventional setup used in this work.

a certain point where these forces equal the surface tension of the solution, the liquid drop becomes a cone, most known as the Taylor cone. At a critical voltage, the repulsive forces overcome the surface tension, which results in the eruption of a jet from the tip of the needle directly to the grounded collector. During the time the jet takes to reach the collector, if the distance between the apparatus and the collector is enough, the solvents that are present in the solution evaporate, resulting in the random deposition of fibers throughout the collector [23], [45].

In order to optimize the functionality and efficiency of membranes regarding the controlled drug delivery purpose, an alternative way of producing fiber mats was explored during this work. Thereby, coaxial electrospinning parameters were studied and analyzed, so that an optimal encapsulation of the model drug used could be achieved. This method is used to prepare double-layered nanofibers with a core-shell structure. In terms of functioning, the theoretical concepts behind coaxial electrospinning are the same as for the conventional setup, except that in the coaxial setup two separate solutions (core and shell) flow through two different but coaxial needles. The setup used is shown in Figure 2.5B.

To avoid bead-like defects in nanofibers production, several parameters must be considered. In terms of process parameters, the applied voltage is of great importance, as it is strongly related with the resultant fiber diameter and the formation of beads. It directly depends on the polymer-solvent system used. The flow rate chosen has a direct impact on the diameter, fiber mat's porosity as well as on fiber geometry. As mentioned before, the distance between the capillary tip and the collector also affects fibers diameter in an inverse relationship. From process to system parameters, the latter ones are related with polymer concentration, solvent volatility and solution conductivity. They are directly related to the viscosity and surface tension of the solution, the formation ability of the fibers and corresponding surface topographies and fiber size, respectively. In the tables below, a more detailed information about the optimal conditions found to perform each type of electrospinning process is given.

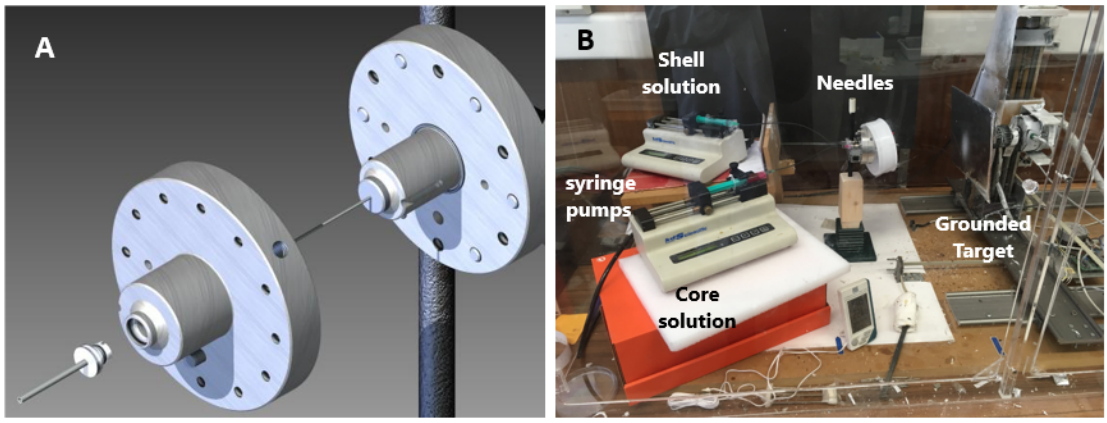

Figure 2.5: Coaxial electrospinning needles detail (A) (adapted from [47]) and coaxial setup used in this work (B).

Table 2.1: Optimal conventional electrospinning parameters obtained.

Needle Gauge	21
Ground Collector Distance [cm]	15
Applied Voltage [kV]	20
Deposition Time [hours]	4
Relative Humidity [%]	30-45
Temperature [ºC]	20-23

Table 2.2: Optimal coaxial electrospinning parameters obtained.

	Core	**Shell**
Solution	RhB:H2O	CA:acetone:DMAc
Syringe Volume [ml]	2	5
Flow rate [ml/h]	0.06	0.4
Needle Gauge	15	11
Grounded Collector Distance [cm]	12	
Applied Voltage [kV]	19.5	
Deposition Time [hours]	2h30	
Relative Humidity [%]	35-40	
Temperature [ºC]	22-24	

To produce the fibers, in both configuration types, a syringe pump (KDS100) was used to control the flow of the solution through the needle, that in the case of conventional setup (ITEC, Iberian Technical, Lda., 21G) was at the constant rate of 0.2 mL/h for a syringe (B.Braun) of 1ml and, for the coaxial setup (Double Layer Coaxial Needles, Linari Engineering) was at a core/shell rate of 0.06/0.4 mL/h, for syringes of 2/5 ml, respectively. While the syringe pumps were responsible for squeezing out the polymer solutions at a controllable speed through the needles, a high voltage was being applied (using a Glassman High Voltage Power Supply) between the needle and a grounded static collector,

coated with an aluminum foil.

2.2 Membranes Functionalization

In the following section, a look over the polymer used to functionalize the membranes obtained via electrospinning will be given. It mentions the advantages of using such polymer and the procedure that was adopted throughout the experimental work to carry out the polymerization.

- **Materials**
  - **Polypyrrole (PPy)**

Polypyrrole is one of a series of heterocyclic polymers which has attracted much attention due to its characteristic electric and electronic properties [48] . Its high conductivity, biocompatibility and low-cost process turn PPy into a very interesting polymer to functionalize the membranes mentioned in the previous section. Furthermore, its usage in several previous controllable drug delivery studies contributed to choose PPy as the conductive polymer to be used in the current work.

- **Methods**
  - ***In situ* oxidation of Pyrrole in aqueous solution**

Dried membranes obtained whether by conventional or coaxial electrospinning with approximately 3 cm x 2 cm of dimensions were coated with PPy through *in situ* oxidative polymerization. The functionalization process consisted in the use of Pyrrole (C_4H_5N, Sigma-Aldrich, M_w = 67.09 g/mol, 98% assay) as the monomer and Iron (III) chloride hexahydrate ($FeCl_3.6H_2O$, Sigma-Aldrich, M_w = 270.30, 98% assay) as an oxidizing agent, in a 2:1 ratio. This ratio resulted from the optimized studies performed by Baptista and coworkers in their work about organic batteries made upon cellulose-based electrospun fibers. [27]

To initiate the functionalization, a 20 ml aqueous solution of 0.05 M of pyrrole was prepared and was left stirring for 10 minutes. Then, the dried membranes with dimensions mentioned above were added and stirred for another 10 minutes, so that they could be soaked with the monomer. The polymerization step started by adding 0.134 g of the monomer to the solution and within a few minutes the membranes started to get black, confirming the formation of PPy. The solution was stirred for 45 minutes, in order to get a fully polymerized membrane. The final step consisted in a thoroughly wash of the membranes, with distilled water and ethanol, so that all the by-products and residues resultant from the reactions occurred could be extracted. To complete the process, the membranes were left drying at room temperature.

2.3 Characterization Methods

- **Morphological Characterization**

Morphological characterization was important in the present work not only to characterize, logically, the morphology of the fibers obtained, but also to measure their diameters and compare the different types of membranes obtained throughout the work. These might include whether the fiber mat contained bead-like defects, if the polymerization occurred uniformly through all the membrane, if the release tests affected the fibers morphology, among others.

  - **Optical Microscopy**

The optical microscope is the traditional technique of microscopy, allowing the study of certain samples up to the micro and even sub micrometer scale. Comparing to other microscopy techniques, this one takes advantage on the much easier handling and samples preparation that is needed to perform the task, but having the scale limitation that other methods do not have. In the work presented, despite the main topic covered being nanofibers, the use of the optical microscope, model Leica DMi8, was justified by the high fluorescence levels of Rhodamine B. By exploring the filters present in the microscope, one in specific had excitation and emission values near the same range as the model drug itself (excitation: 554 nm; emission: 580 nm), as shown in Figure 2.6. Given the suitability of the RHOD filter, its use enabled the verification of whether the Rhodamine was present in the membrane. Moreover, a more general observation over the fibers morphology, the presence of bead-like defects, among other characteristics, could be done, clearly without the same magnification as the ones obtained by the Scanning Electron Microscopy technique, for example.

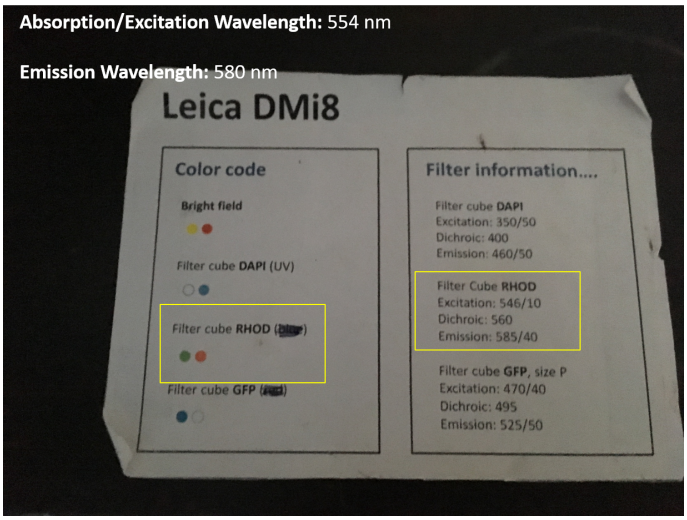

Figure 2.6: Similarity between values of RhB and the Leica RHOD filter.

- **Scanning Electron Microscopy (SEM)**

SEM is a technique that allows the collection of high-resolution, high-magnification images of the samples analyzed. In a general and more brief way of looking at SEM's functioning process, it uses a narrow electron beam to scan a certain area of the sample. From the interaction between the beam and the atoms of the sample involved, it results the emission of low-energy secondary electrons (1-20 eV). The intensity of this emission is, thereby, a function of the atomic composition of the sample and the geometry of the sample's piece that is being observed. Due to the narrowness of the excitation beam, the resultant beam has a high depth-of-field that, otherwise, could not be obtained by a common optical microscope.

In the work hereby presented, samples were prepared by cutting some pieces of different types of membranes, varying either in the type of production method (conventional or coaxial electrospinning) and in several conditions related to controlled release tests (namely, before stimuli application and after stimuli application for both types of polarity). Then, they were placed on a metallic sample support by means of a conductive carbon strip. The model used to perform the technique was the JEOL 7001 and the resulting images were analyzed using ImageJ® image processing software.

Additionally, a histogram analysis is made relating the different fiber diameters registered for each sample with the relative frequency with which they exist in the piece of sample analyzed. The diameter measure of the fibers was performed with ImageJ® software, considering 50 different measurements for each sample (10 measurements for each of the most superficial 5 fibers).

- **Electrical Characterization**

  - **Electrical Conductivity**

The membranes produced right after electrospinning process, because of their composition (mainly cellulose acetate and a much less amount of drug), are considered non-conductive. That is the reason why their functionalization is required, in order to turn them into electro-stimuli responsive membranes, so that the controlled delivery tests can be performed.

Electrical characterization takes part in this work right after the PPy polymerization step, to measure the conductivities of the membranes before subjecting them to an electric stimulus. That same conductivity values will then be compared to the ones obtained after the controlled release tests have been performed, from where conclusions can be taken on the effects that the stimulus had on the membrane's conductivity.

The conductivities measurement process is performed with resource to a Picoammeter/ Voltage source (Keithley Series 6400 Picoammeters) and a computerized microprobe (Alessi REL-450) with two positioners. The setup used is depicted in Figure 2.7.

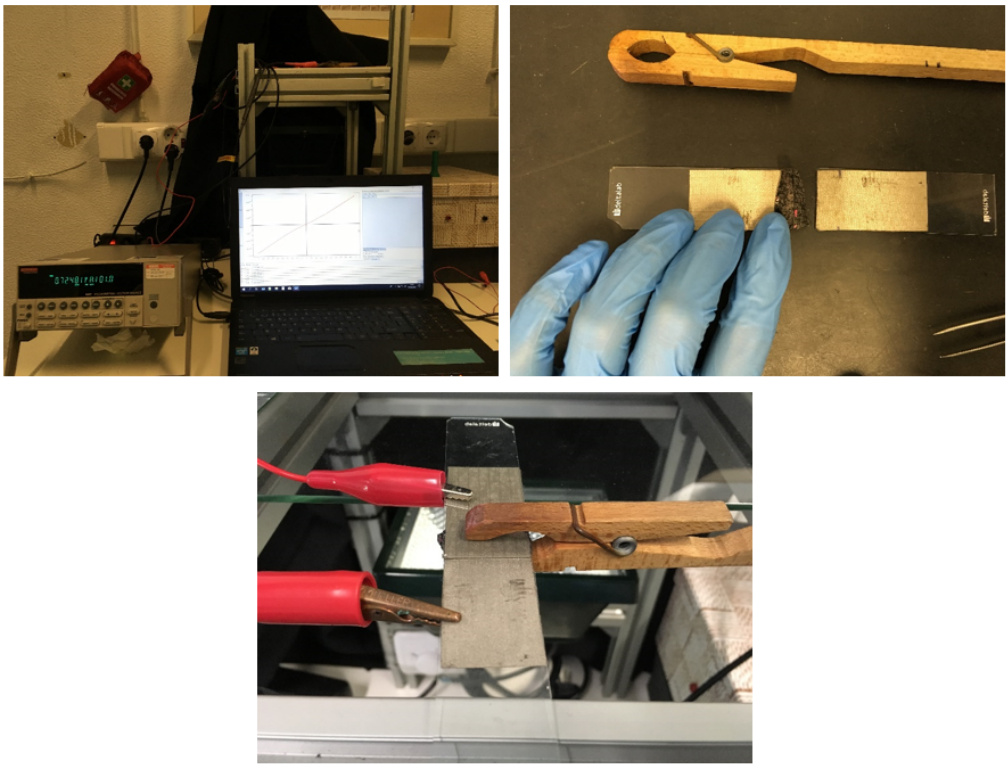

Figure 2.7: Conductivity measurements setup. Upper left figure: overall setup; Upper right and lower figures: illustration of the transversal measurement setup, with a detail over the positioning of the membrane in the microscope slides and its pressing between two conductive carbon foils.

As a result of each measurement, either in the planar or transverse planes, a Current-Voltage Characteristic Curve (*I-V* Curve) is obtained. This type of curves shows the relationship between the current flowing through an electronic device and the applied voltage across its terminals. According to Ohm's law,

$$V = RI \tag{2.1}$$

Which states that the slope of the straight line that represents the current (I) against the potential difference (V) is equal to 1/R (in the case of an ideal resistor). Thereby, by obtaining the *I-V* Curves and sorting out the resistance (R), the functionalized membrane's conductivity, σ in Siemens per centimeter (S/cm), can be obtained by applying the following equation:

$$\sigma = \frac{l}{AR} \tag{2.2}$$

Where l represents the length of the piece of material, A represents the cross-sectional area where the current has passed-through, and R represents the resistance.

Conductivity was measured and compared in both planes (transverse and planar), being the transverse plane measured by pressing a membrane of 2,5 x 1 cm between two

microscope slides, coated with conductive foils of carbon (setup is depicted in 2.7). As for the planar measure, membranes were cut and immobilized on microscope slides with conductive glue, like represented in Figure 2.8. In the case of the transverse measurement, the cross-sectional area corresponded to the area of the slide where the membrane was inserted into; as for the planar setup, this value was obtained by multiplying the distance between electrodes (1 cm) by the corresponding membrane thickness. Functionalized membranes resulting from both conventional and coaxial electrospinning setups were analyzed.

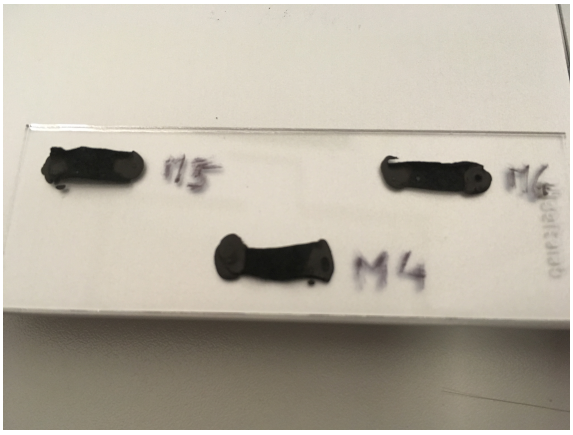

Figure 2.8: Planar conductivities samples preparation. Three distinct membranes are cut into similar size pieces and glued against a microscope slide with a conductive glue. Measurements are performed between the two edges of the membrane, i.e, between the two glue spots.

2.4 Controlled Drug Delivery Tests

After membranes production and corresponding functionalization, the simulation and analysis of the drug release behavior was performed. In a general approach to this topic, the membranes are first inserted into a recipient with water, being then subjected to a potential difference, between the membrane and an electrode, corresponding to the electrical stimulus. Applying the stimulus during a certain period, repeating it several times in a determined sequence, gives rise to a controlled drug release study. After each stimulus, the absorbance of the medium is measured, using the UV-Vis Absorbance Spectroscopy technique. Correlating the values obtained with the resultant equation that emerges from a previous performed calibration curve, an approximation of the amount of drug that was released after each stimulus can be done. Once known the amount of drug released, different types of data processing can be made, such as a cumulative drug release graph in function of time.

– UV-Visible Spectroscopy

UV-visible spectrometers can be used to measure the absorbance of either ultra violet or visible light by a sample. In the work presented, the range analyzed went through both types of radiation, from 190 nm to 900 nm.

Inside a spectrometer, a light source emits a beam of white light. This beam then goes through a monochromator and is focused onto a diffraction grating that can split the incoming light into its different component colours. The diffracted beam than goes by a beam splitter, which splits the beam towards the two cells or cuvettes. One of them, the reference cell, also called blank, contains the solvent in which the sample is dissolved; the other one, the sample cell, contains the sample that is pretended to be analyzed.

The intensity of light passing through both the reference cell (I_0) and the sample cell (I) is measured by the detectors. If I is less than I_0, it means that the light was absorbed in the cuvette that contains the sample. The absorbance value (A) is related to these intensities by the following equation:

$$A = \log_{10} \frac{I_0}{I} \tag{2.3}$$

During the experimental work, 3 ml of distilled water were used to correct the baseline of the equipment (PG Instruments Ldt., T90+ UV/VIS Spectrometer). After each stimulus application, the absorbance was measured and plotted for each wavelength, using UVWin Spectrometer Software.

As mentioned above, in order to know the concentration of RhB released, a previous calibration curve had to be done. This relationship is explained by the Beer-Lambert Law, which states that the absorbance is proportional to the concentration of the substance in solution, expressed in the form of the following equation:

$$A = \epsilon c l \tag{2.4}$$

Where:

A = absorbance

I = optical path length, i.e. dimension of the cell or cuvette (cm)

C = concentration of solution (mol dm^{-3})

ϵ = molar extinction, constant for a particular substance at a particular wavelength (dm^3 mol^{-1} cm^{-1})

Thereby, if by plotting a range of absorbance values in function of known concentrations, a linear relationship is obtained, as theoretically expected by the Beer-Lambert Law, such graph can be used as a calibration curve.

– Calibration Graph

An initial study of how absorbances of RhB in water vary with different drug concentrations is needed in order to understand and further analyze the results obtained in the controlled release tests.

To obtain the calibration curve, solutions with varying concentrations were prepared. From a stock solution of 0,6 mM of RhB in water, other concentration values were obtained by diluting that high concentrated solution. The prepared solutions are listed in Table 2.3 and their colour change pattern is shown in Figure 2.9. The different absorbances were measured, the plots were analyzed, and a calibration curve was done.

Table 2.3: Concentrated solutions used in the calibration curve

Rhodamine B in water calibration curve concentrations [mM]									
0.001	0.002	0.003	0.005	0.006	0.008	0.010	0.015	0.020	0.025

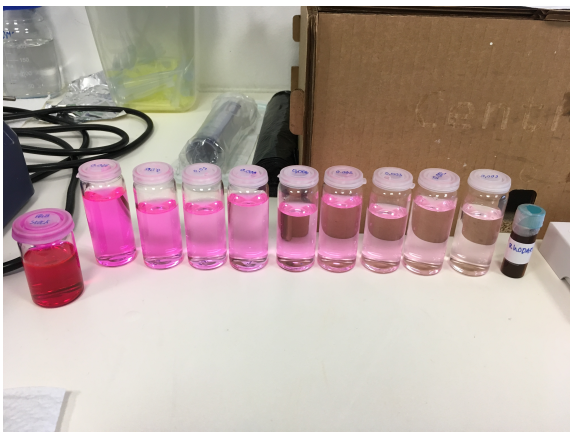

Figure 2.9: Colour difference between different concentrated solutions. The red solution corresponds to the stock solution.

– Diffusion Drug Tests

Since the model drug used, RhB, is water-soluble, it is important to analyze how much of the drug is released by normal diffusion, only by being immersed in water. This study is even more important if we consider that during the polymerization step, membranes are totally immersed while being coated with PPy. Furthermore, to clearly identify how much of RhB is released only due to the stimulus, an idea of how much rhodamine is released just by immersing a functionalized membrane in water is mandatory.

To perform this task, a recipient is filled with 20 ml of distilled water and, for the case of an uncoated membrane, this one is fully immersed in water, being the absorbances measured in specific time intervals. The same procedure is taken for the case of PPy coated membranes, with the difference that only the same portion of membrane that is immersed into water in the controlled released tests is inserted in water during the assay.

– **Drug Controlled Release Tests**

The setup used to perform the drug-controlled delivery tests is depicted in Figure 2.10. A recipient is filled with 20 ml of distilled water, where a functionalized membrane is immersed with a silver electrode. To avoid unnecessary variations between measures, it is important to keep the distance between the electrode and the membrane throughout every test. The membrane is connected to the positive pole of a high voltage supplier (Keithley 237 High Voltage Source Measure Unit) and the electrode is connected to the negative pole. Each test is made up by several stimuli application times, with the same polarity but with different values, for each type of membrane.

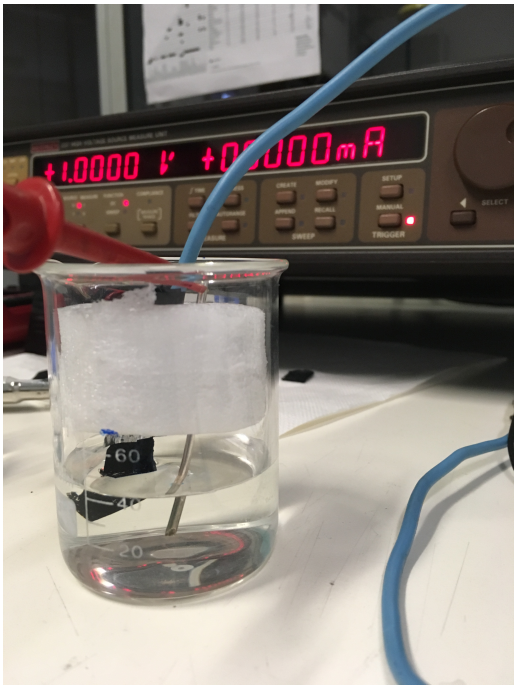

Figure 2.10: Controlled drug release setup. Part of the membrane is immersed and connected to the positive pole of the voltage supplier and is placed in a constant distance from a negatively charged silver electrode.

Every sample is immersed in a new medium for each new test. During a test and after application of a stimulus, the apparatus (membrane and electrode) is removed from the water, 3 ml of the medium are withdrawn and measured in UV-Vis Spectroscopy and then returned to the same solution.

Both types of membranes (from conventional and coaxial electrospinning) were tested through positive and negative stimulus (in the range of 1 V to 5 V, during 1 - 5 minutes), being also studied the condition of 0 V, to understand whether it would impact the drug release and if there was any difference comparing with the normal diffusion tests.

Chapter 3

Results and Discussion

In the chapter hereby presented, the results obtained throughout the experimental work will be shown and discussed. A detailed analysis over the different techniques mentioned in the previous chapter will be done, starting with the morphological characterization of the produced and functionalized membranes. This section also presents in detail the results obtained for the controlled drug delivery tests.

3.1 Production and morphological characterization of electrospun membranes

From a technological point of view, conventional electrospinning can be considered to be easier and faster, since it just needs a blend between the desired drug and the polymer and a few parameter adjustments. However, as stated in previous chapters, this electrospinning method has several side effects, such as the homogeneous drug distribution in the overall fiber and the consequent burst release effect, which might turn to be harmful to the patient [15].

Given the unique advantages that coaxial electrospinning offers compared to the conventional setup, mainly in terms of a better drug encapsulation and the significant attenuation of the burst effect, the main goal of this work, right in its beginning, was to explore and optimize nanofiber production via this latter method.

Therefore, and starting by pumping into the core a solution of 0.6 mM of Rhodamine B in water, together with a 12% (w/w) CA solution, several attempts were tried, and none worked. The process was unstable, and it was not verified any uniformity in the resultant membranes. Several flow rate combinations were attempted and distance to collector was altered too, as well as different values of the applied voltage (in a range between 15kV -

20 kV). One possible reason to justify such difficulty in obtaining uniform membranes could be the excessive amount of water that was being put into contact with CA. To clarify this situation, a more concentrated solution of Rhodamine B (1.5 mM) was tried instead of the 0.6 mM solution, in an effort to reduce the amount of water directly in contact with cellulose acetate. Since the results did not changed substantially, instead of dissolving Rhodamine B in water, the dye was dissolved in the same amount in ethanol. The only condition that inhibited ethanol of being chosen as a preferential solvent was its considerable miscibility with cellulose acetate. This miscibility would have the negative effect of a weaker drug encapsulation capacity (compared with water), thus enabling more drug to get released by diffusion. In the opposite logic, the immiscibility that characterizes water-cellulose acetate relationship was the reason that led to use water as the solvent in the process, looking forward to a better encapsulation of the model drug. In Table 3.1, the combinations that were attempted throughout the work are listed.

Table 3.1: List of combinations attempted during the coaxial electrospinning process.

Cellulose Acetate (w/w) [%]	Rhodamine B [mM]	Solvent	Flow Rates Combinations (Shell-Core) [mL/h]	Observations
12	0.6	Water	Several from 0.06-0.01 to 0.6-0.06	No uniform membrane
12	1.5	Water	Several from 0.05-0.01 to 0.8-0.06	No uniform membrane
18	0.6; 1.5	Water	Several from 0.05-0.01 to 0.5-0.08	No membrane obtained
12	0.6	Ethanol	Several from 0.05-0.01 to 0.8-0.08	No uniform membrane
8	**0.6**	**Water**	**0.4 - 0.06**	**Uniform and continuous membrane**

As it can be stated from Table 3.1, the only combination that was able to produce a uniform and continuous membrane was the last one, with a lower cellulose acetate concentration. As seen in images obtained via Optical Microscopy (Figure 3.1) and as it would be expected, this mentioned combination does not allow a perfect and defect-less membrane production, but it was the only option that enabled the coaxial process to be used throughout the practical work. Since no other study using the same carrier-drug

combination as the one used in this work was found in the literature, a more exhaustive and exploratory work had to be done to find the desired conditions. The starting point to do so were the conditions used in previous studies using the same drug model, namely [32], [49], [50].

Parallel to this work, in order to get a comparison alternative for the coaxially electrospun membranes, a conventional setup was used as well. Oppositely to the coaxial process, in the conventional method only one solution is electrospun through the only needle that exists. Therefore, in this case, Rhodamine B was incorporated in the cellulose acetate solution preparation. The same concentration (0.6 mM) that was diluted in water for the coaxial setup, was diluted in the acetone:DMAc solvent mixture used in the production of CA. The first conditions tried were the same as those used to electrospin a typical solution of cellulose acetate [23]. Those conditions were the optimal result of a complete exploratory work, thereby reducing the time consumed in this work to do so, like it was done for the coaxial electrospinning. Once again, 8% (w/w) CA was used, which had the advantage of enabling a continuous and uniform membrane to be obtained, but at the same time, its low viscosity might has led to the presence of some defects in the resulting fibers (Figure 3.1).

Despite the orders of magnification are not enough to reach the nanofiber level, Optical Microscopy technique, as mentioned in the Materials and Methods chapter, was a technique employed in this work to verify whether the membranes that were being produced contained Rhodamine B. This was possible due to its high fluorescence level (excitation/emission wavelengths - 554 nm/580 nm) and by the similarity between absorption/excitation values of RhB and the RHOD filter of the microscope (Optical Microscopy sub-section, previous chapter). An example of the type of images obtained is depicted in Figure 3.1. As expected, the strong fluorescence property of RhB, denoted by the higher brightness in the images, is an indicator that the fibers being produced contain the model drug.

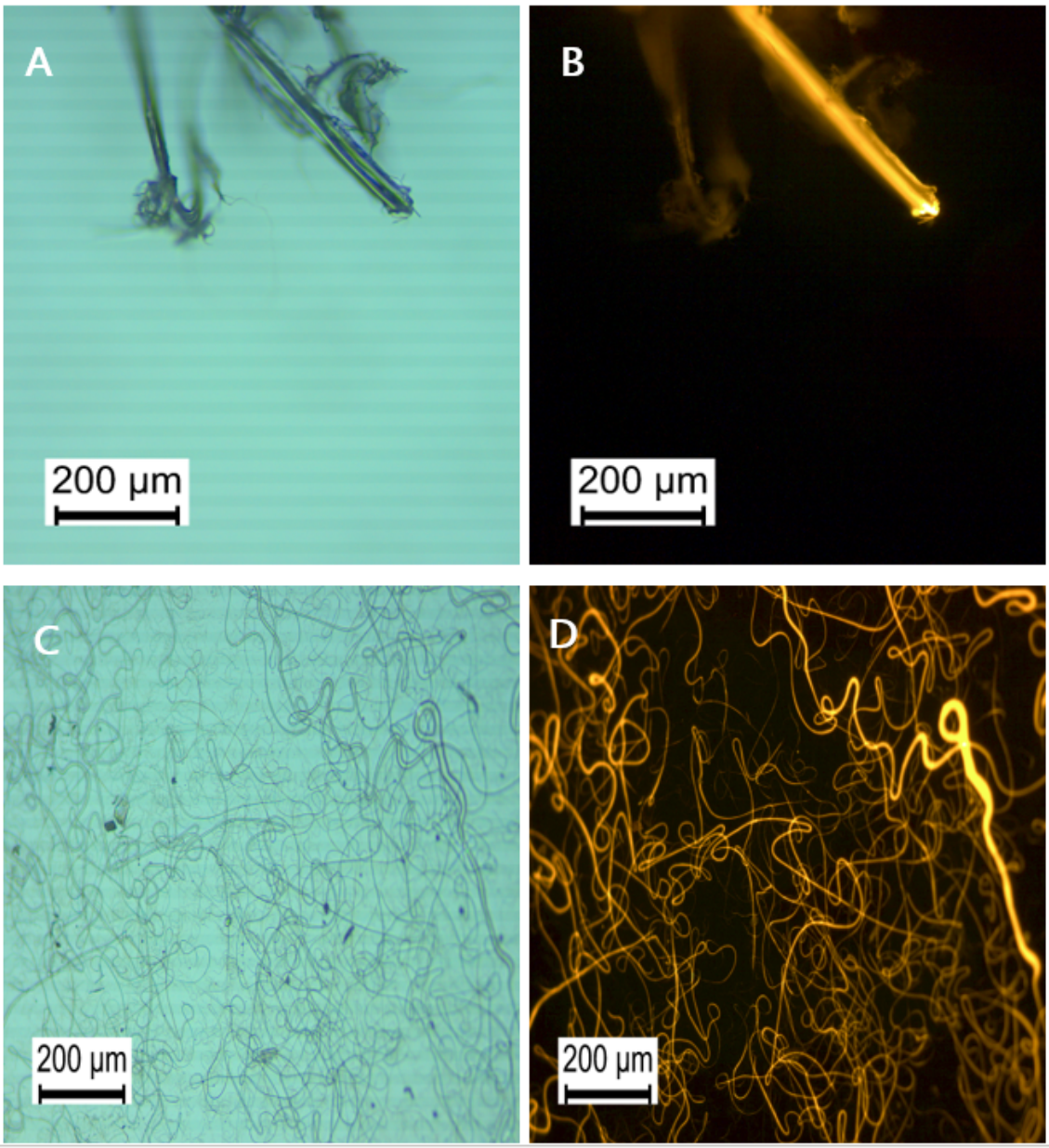

Figure 3.1: Optical Microscopy images (Bright Field filter - left; RHOD filter - right). A and B correspond to fibers obtained via coaxial setup and C and D to the ones produced via the conventional setup.

Figures A and B depict an individualized fiber produced using a coaxial electrospinning process showing a uniform brightness. On the other hand, Figures C and D, present several fibers produced using a conventional electrospinning setup. A detailed analysis over these and other images with different magnifications leads to the observation of bright dots spread all over the membrane. The presence of these bright spots can be explained by a non-uniform dispersion of Rhodamine within the fibers or due to beads formation during the electrospinning process - either in conventional or coaxial setup – probably caused by the low viscosity of the solution.

Besides some difficulties in obtaining a stable and reproducible ES process, the selected ES parameters for both setups allowed the production of fibers with encapsulated RhB.

Later, SEM analysis was carried out for a detailed morphological characterization of the produced electrospun membranes. Figure 3.2 presents the SEM images of CA fibers and CA + RhB fibers produced via conventional and coaxial ES setup.

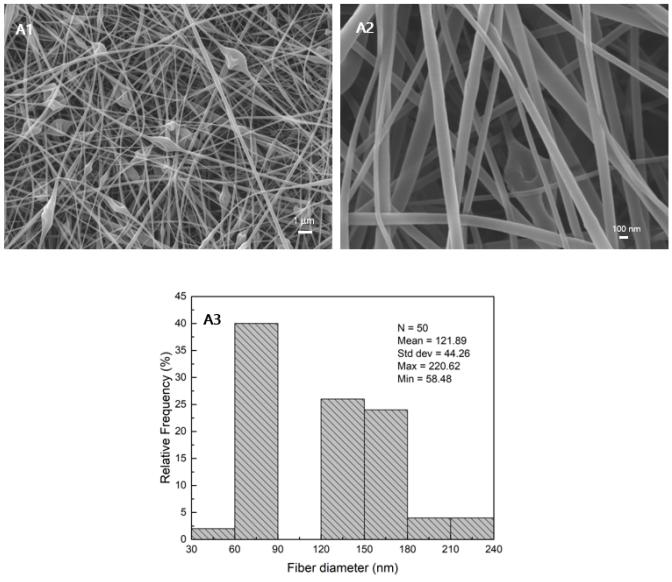

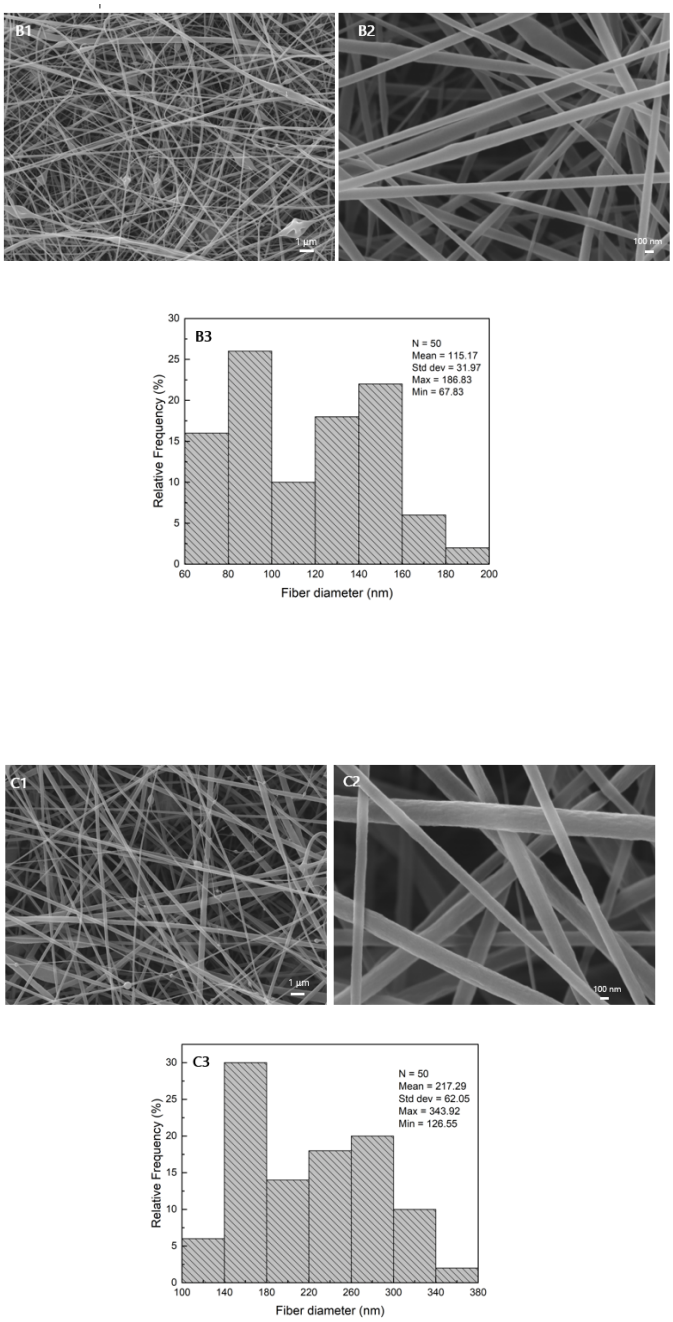

Figure 3.2: SEM images and corresponding histogram for fiber diameter analysis. Number 1 of each set corresponds to a magnification of x5000 and number 2 to a magnification of x30000. First set of pictures (A) corresponds to CA fibers (8% wt). Set B to CA+RhB produced by the conventional electrospinning setup. Set C to CA+RhB obtained via coaxial electrospinning.

In general, the SEM images presented in Figure 3.2 show randomly orientated electrospun fibers with a high fiber diameter distribution. Cellulose acetate electrospun fibers (Figure 3.2A) clearly present a bead-like morphology due to the low viscosity of the polymeric solution. After RhB encapsulation within fibers using conventional ES setup (Figure 3.2B), it is clear that fiber morphology does not significantly change. This

bead-like morphology may explain the presence of the bright spots previously mentioned.

Using the coaxial setup to encapsulate RhB (Figure 3.2C), the electrospun fibers showed a higher average diameter and a rough surface. The larger diameters are due to the larger gauge of the outer needle used for coaxial setup when compared with the conventional one - as previously stated in Tables 2.1 and 2.2 of the Materials and Methods chapter. The surface roughness can be probably explained by the interaction of cellulose acetate molecules in the shell with the water molecules embedded in the core (containing RhB).

Interestingly, membranes produced by both types of electrospinning setup showed similar values in terms of membrane thickness. In the case of the conventional setup, resultant membranes had an average thickness of 0.051 ± 0.013 mm, and the ones electrospun via the coaxial setup resulted in an average thickness of 0.059 ± 0.031 mm.

3.2 *In situ* oxidative polymerization of Py

After membranes production, in order to turn them into electro-stimuli responsive membranes, they were coated with PPy through *in situ* oxidative polymerization. Polypyrrole is among various conjugated polymers that are under academic and industrial interest due to their potential application as bioactuators, biosensors and stimuli-responsive drug controlled systems [51], [52], [53]. Fibers functionalization with PPy can be performed through two different methods: by *in situ* vapor-phase polymerization of Py or by *in situ* Py oxidative polymerization. Baptista et al [23], [27] studied the functionalization of cellulose acetate fibers with PPy using both methods. The first important conclusion withdrawn from the study was that *in situ* vapor-phase polymerization resulted in brittle composite fibers. Therefore, and given the good results obtained by the oxidative polymerization, a more detailed study on this method was performed and they came up with the most adequate conditions to obtain PPy-coated CA fibers. In Table 3.2, these optimal conditions are listed.

Table 3.2: List of most adequate conditions for *in situ* oxidative polymerization of Py [27].

Py concentration [M]	**Oxidant/Monomer ratio**	**Reaction Time [min]**
0.05	2	30

Additionally to what has been explained in the Materials and Methods Chapter in section 2.2, an adjustment to the conditions listed in Table 3.2 had to be done. The 30-minute reaction time proven to be short to fully polymerize the fibers used in the current work. Instead, a 45-minute reaction under constant stirring was applied, inducing significant visual changes in the resultant membranes. This difference is depicted in Figure 3.3 below.

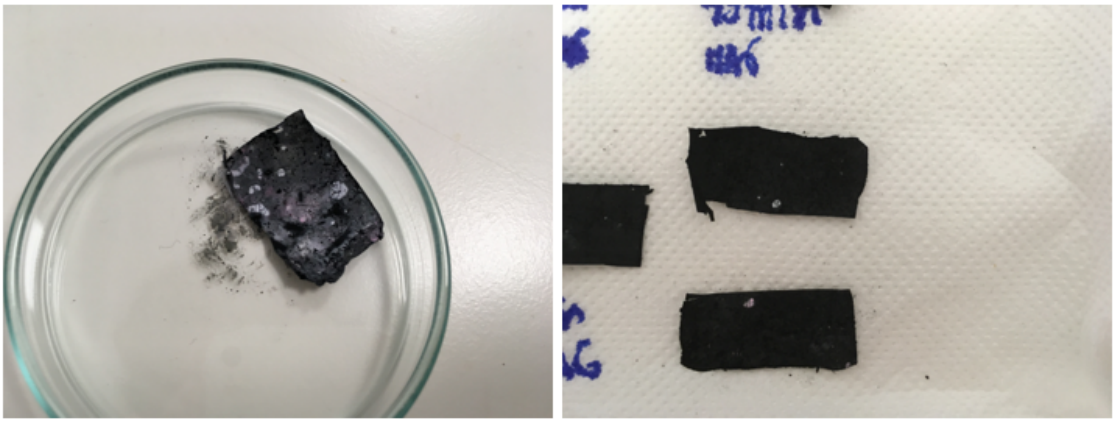

Figure 3.3: Differences between a 30-minute (left) and a 45-minute (right) polymerization membrane. The 45-minute polymerized membranes shown a most uniform PPy coating when compared to the 30-minute one.

Figure 3.4 comprises both types of membranes, the ones obtained by conventional electrospinning and the others by the coaxial technique, where the pink color is clearly visible in the case of the conventional setup (a similar result was obtained in [31]). It also compares and highlights the difference between membranes before and after the polymerization phase.

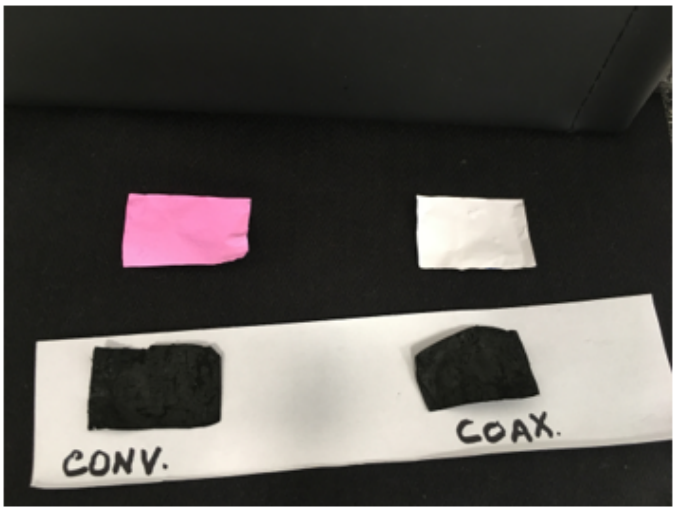

Figure 3.4: Comparison between membranes before and after functionalization with PPy. Pink-coloured conventional membrane highlights the homegeneous distribution of RhB along the fiber matrix. Coaxial membranes, on the other hand, present a more heterogeneous distribution, with the RhB suspected to be highly concentrated on the fibers core.

Since the polymerization method used involves the immersion of the membrane in an aqueous solution, it was important to estimate the amount of the model drug that would leave the CA mat by diffusion during this time. Detailed information on this topic will be presented in the following section of this chapter.

To analyze and understand the morphological changes subsequent to the polymerization phase, SEM images were obtained for a coaxial polymerized membrane, serving this example as a representative approach to all the membranes that were functionalized throughout the work.

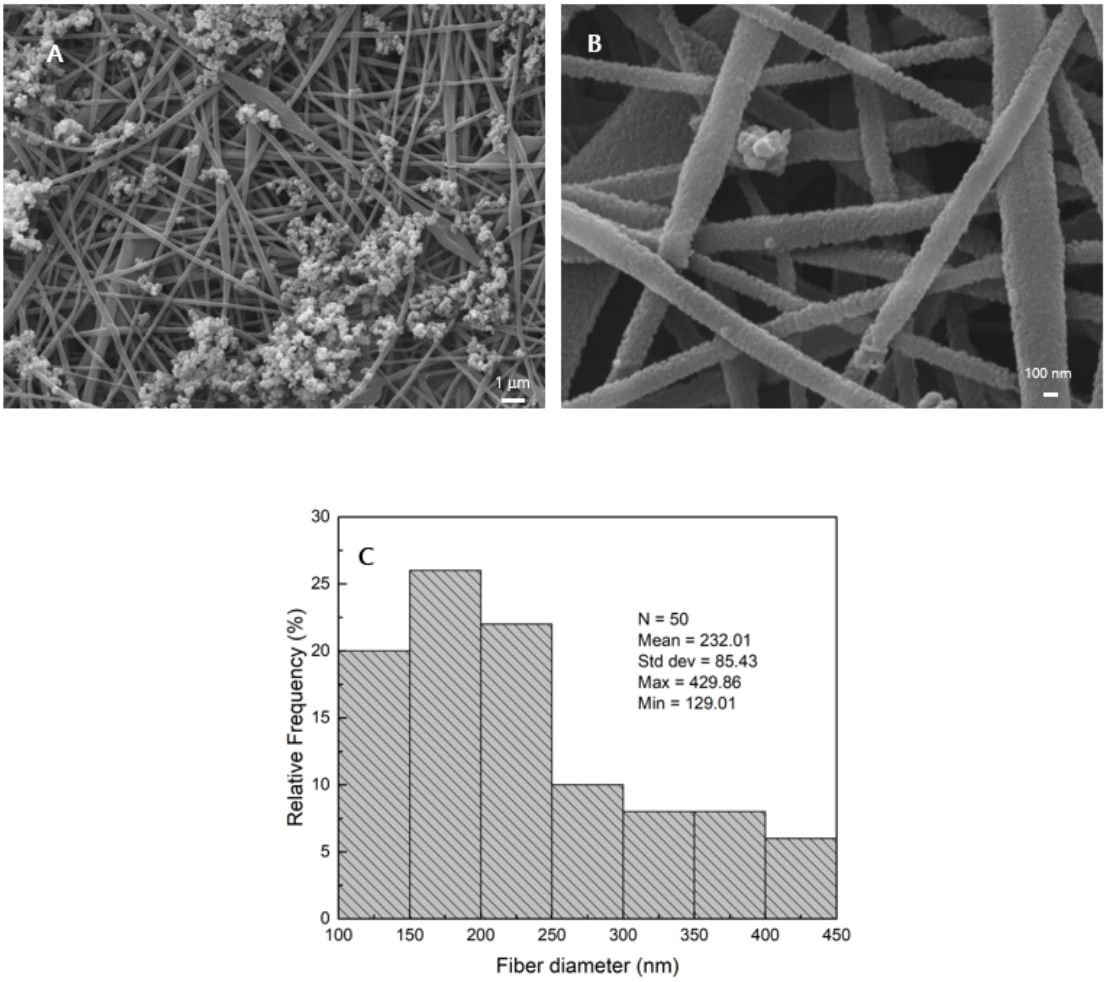

Figure 3.5: SEM images and corresponding histogram for fiber diameter analysis of a coaxial functionalized membrane. A corresponds to a magnification of x5000 and B to a magnification of x30000.

In terms of membrane polymerization, in the higher magnification image (Figure 3.5B), it is visible that the polymer is uniformly distributed along the different fibers, showing some agglomerates at a larger scale. Agglomerates presence must be due to an incomplete washing of the membranes after the polymerization process, being perhaps more strongly adhered to the nanofibers than the other ones.

While, by SEM, a more detailed analysis on morphological changes can be performed, electrical conductivity of the functionalized membranes was measured after the polymerization process to evaluate if they were suitable for electrically stimulated drug release systems.

As stated in the previous chapter, electrical conductivity values were measured in both configurations (transverse and planar) and were obtained through the corresponding I-V curves, being applied a potential difference between -1V and +1V and measured the resultant current values. An example of this type of curve is depicted in Figure 3.6. To minimize errors, each measurement was repeated three times.

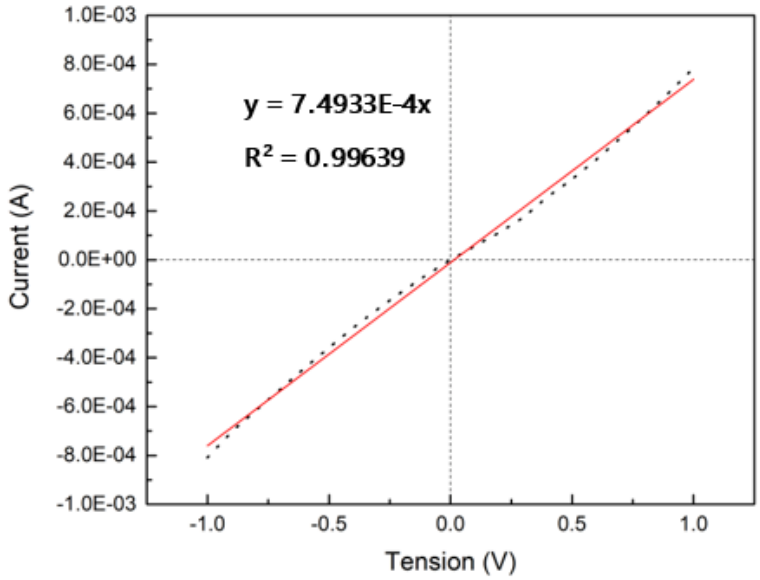

Figure 3.6: I-V sample curve, obtained from a planar measurement in a conventional electrospun membrane.

The conductivity values of the electrospun membranes were determined using equation 2.2. Table 3.3 summarizes the results obtained for the membranes before and after PPy functionalization. The results shown for the case of a membrane before being covered with the conductive polymer (uncoated membrane), were withdrawn from the studies presented in [23].

Table 3.3: Table summarizing conductivities before and after functionalization with PPy.

	Planar Conductivity ($S.cm^{-1}$)	Transverse Conductivity ($S.cm^{-1}$)
ES-conventional/PPy	$(6.03\pm0.03)x10^{-02}$	$(2.84\pm0.05)x10^{-05}$
ES-coaxial/PPy	$(4.81\pm1.23)\ x10^{-02}$	$(2.27\pm1.08)\ x10^{-05}$
Uncoated membrane	$(7.1\pm0.8)x10^{-11}$	

In the planar setup, conductivities are measured between two electrical contacts that are placed in the same plane (membrane´s surface), whereas transverse setup implies that conductivity is measured across the transversal plane (thickness direction) of the membrane. During Py polymerization, the fibers at the surface of membrane are uniformly coated with PPy which contributes to the higher conductivity (~10^{-2} S/cm) using the planar configuration – as verified in Table 3.3. In transverse configuration, fewer contact points between fibers coated with PPy or an incomplete Py polymerization of the inner fibers of the membranes can explain such difference on conductivity values (~10^{-5} S/cm).

3.3 Controlled drug release tests

To estimate the amount of Rhodamine B released during the drug release studies, a calibration curve was performed using solutions of RhB in water with specific known concentration - listed in the Materials chapter. The absorbance obtained for each solution in the UV-visible range is depicted in figure 3.7. As already mentioned, RhB is well known to display absorbance peaks at 190 nm and 554 nm [32], [35], [54]. The calibration curve obtained at 554 nm is presented in figure 3.8.

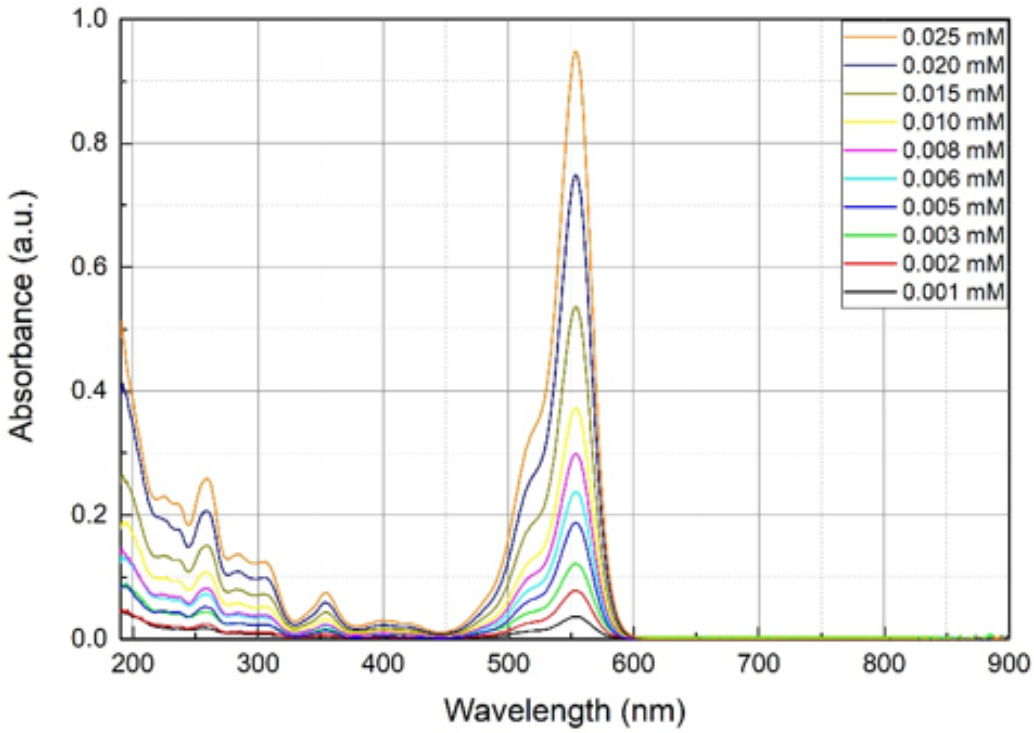

Figure 3.7: Absorbances profiles obtained for the known concentrations of RhB aqueous solutions. It is clear that 554 nm is the wavelenght for which RhB presents higher absorbance values.

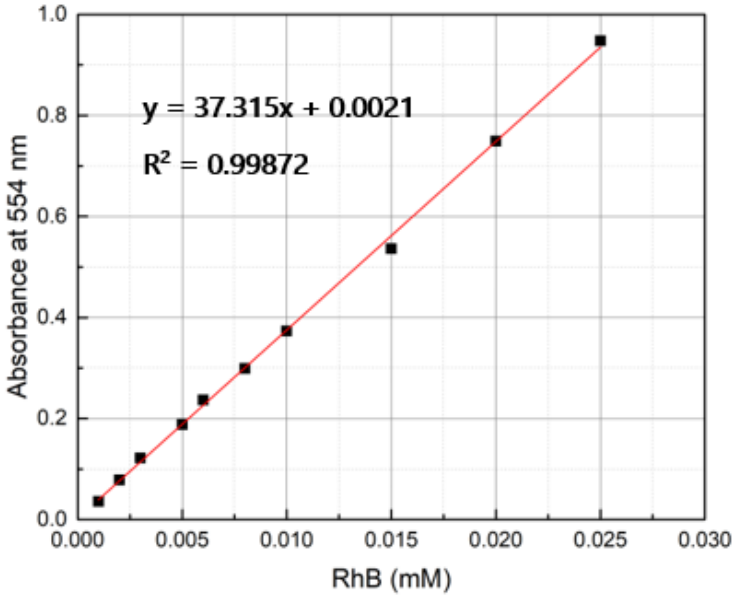

Figure 3.8: Calibration curve, calculated for the absorbances registered in the maximum wavelength peak (554 nm).

As previously explained, before being subject to the controlled drug release tests by application of an electrical stimulus, membranes must first be functionalized with a conductive polymer, to turn them into stimuli-responsive substrates. During the polymerization step, 2 x 3 cm membrane pieces are immersed in an aqueous solution during a certain time interval. During this period, Rhodamine B might be disseminated through the aqueous medium by passive delivery, namely via diffusion. To understand and control how much of the model drug is lost during this period, it is important to simulate such process through a controlled diffusion release study. This study is performed simply by immersing a membrane in a certain volume of water and measuring the corresponding absorbances in specific time instants. Using then the calibration curve depicted in Figure 3.8, the absorbances are converted into concentration units. To obtain the desired drug release profiles, the estimated amount of RhB encapsulated in nanofibers is also an essential parameter to be measured. By dissolving an uncoated membrane in 1 mL acetone solution, due to the high solubility of CA in such solvent, dissolution of the membrane occurs and, after acetone evaporation, only RhB remains. Filling the recipient with a certain volume of water and measuring the resultant absorbance, the amount of Rhodamine B previously encapsulated can be estimated.

Therefore, the percentage of Rhodamine B released is obtained by the following equation:

$$\%\ of\ RhB\ released\ =\ \frac{mM\ of\ RhB\ measured}{mM\ of\ RhB\ encapsulated} \times 100 \tag{3.1}$$

Figures 3.9 and 3.10 present a representative example of the results obtained for the controlled release of RhB by normal diffusion for the conventional and coaxial membranes.

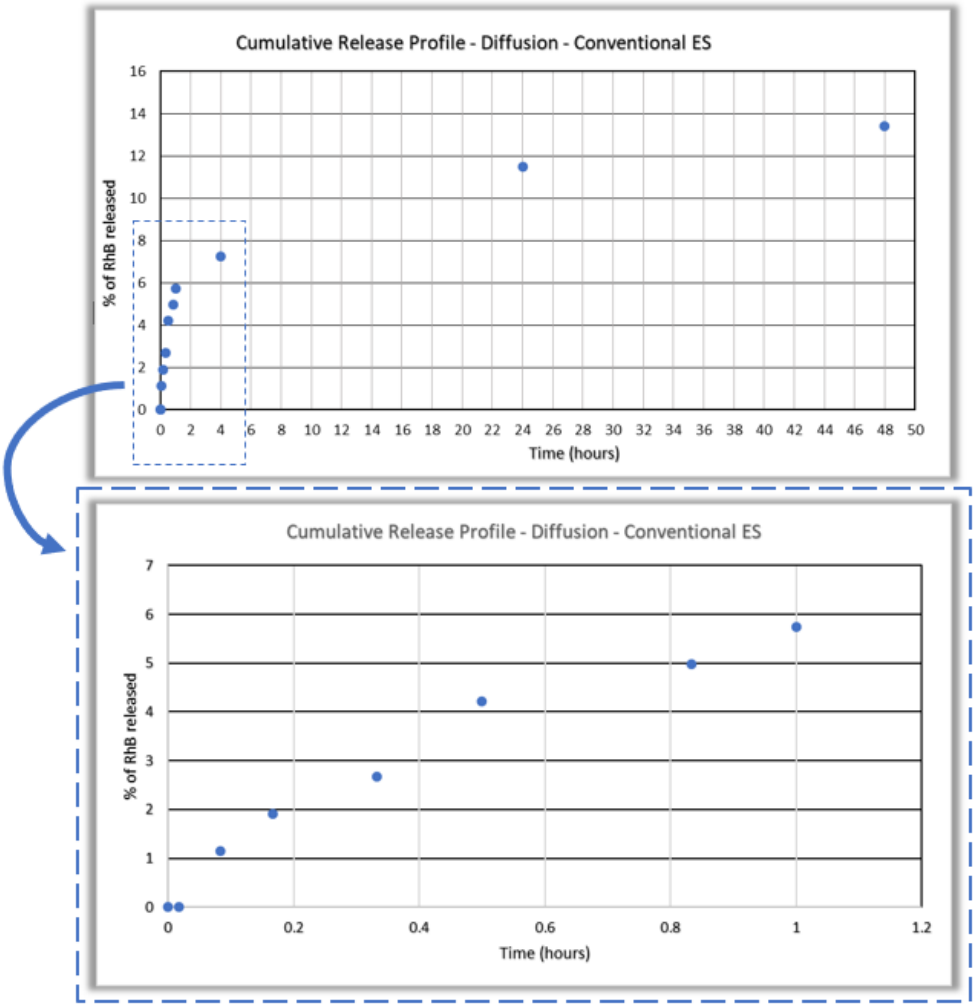

Figure 3.9: Cumulative release profile via diffusion for the case of a conventional uncoated membrane. Absorbances were measured after 1min, 5min, 10min, 20min, 30min, 50min, 60min, 4h, 24h and 48h membrane had been immersed.

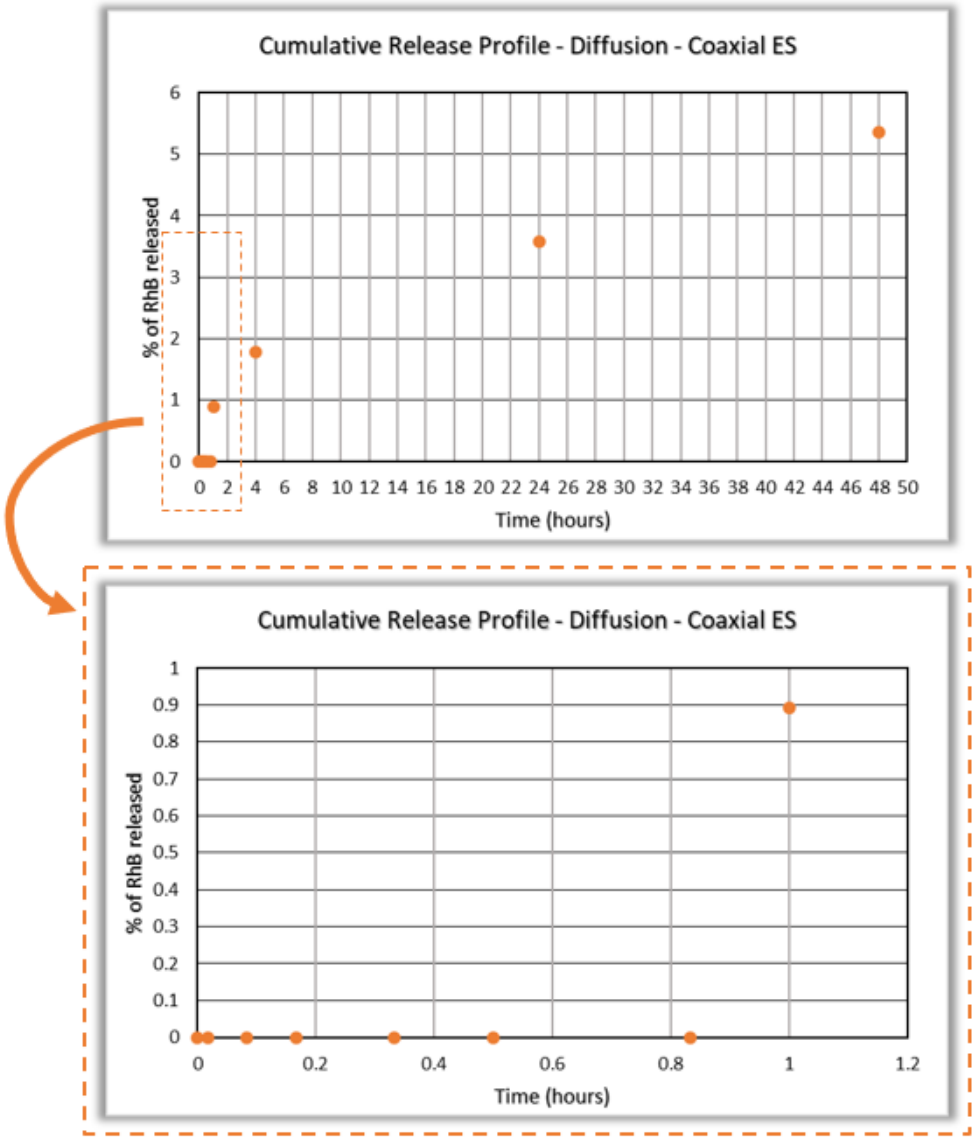

Figure 3.10: Cumulative release profile via diffusion for the case of a coaxial uncoated membrane. Absorbances were measured after 1min, 5min, 10min, 20min, 30min, 50min, 60min, 4h, 24h and 48h membrane had been immersed.

As it can be stated by comparing both figures, percentage of RhB released reaches higher values for the case of the membrane produced by conventional electrospinning. This difference was expected due to the inhomogeneous drug distribution in the overall fiber that characterizes fibers obtained via the coaxial setup. It means that, in the case of the coaxial membranes, RhB is probably more concentrated in the fibers interior, driven from the way fibers are produced, whereas for the case of the conventional electrospun membranes, drug presents an higher surface distribution. Despite the mentioned differences, one common conclusion that can be withdrawn from analysis of both profiles is the

overall low percentages of the model drug that get released during the time interval considered. Looking carefully to the total amount of time consumed by the polymerization step (approximately 55 minutes), during which membrane is immersed in an aqueous solution, for both types of membranes, the percentage is considerably small. This means that, after being polymerized, the majority of the model drug is still encapsulated, enabling further studies on controlled release by application of an external stimulus.

Since the final goal of this thesis is to electrically stimulate the obtained membranes and then analyze its responsive behavior, the expectation is to obtain a certain drug release profile, ideally with the drug diffusing out of the membrane earlier than what was verified for the diffusion study mentioned above. However, before starting the stimulated controlled release study, a similar logic as the one explained above is needed. Thereby, if a study of the percentage of RhB released during the functionalization of the membranes was necessary, so it is in the case of understanding how the functionalized membranes will behave when immersed in water during the electrically controlled studies. Studying the diffusion of the model drug in this case is crucial to clarify, after applying the stimulus and measuring the absorbances, how much of the RhB is released via diffusion or by application of the electrical stimulus.

The following figures present the drug release profiles, only by diffusion, of both types of membranes coated with conductive polymer.

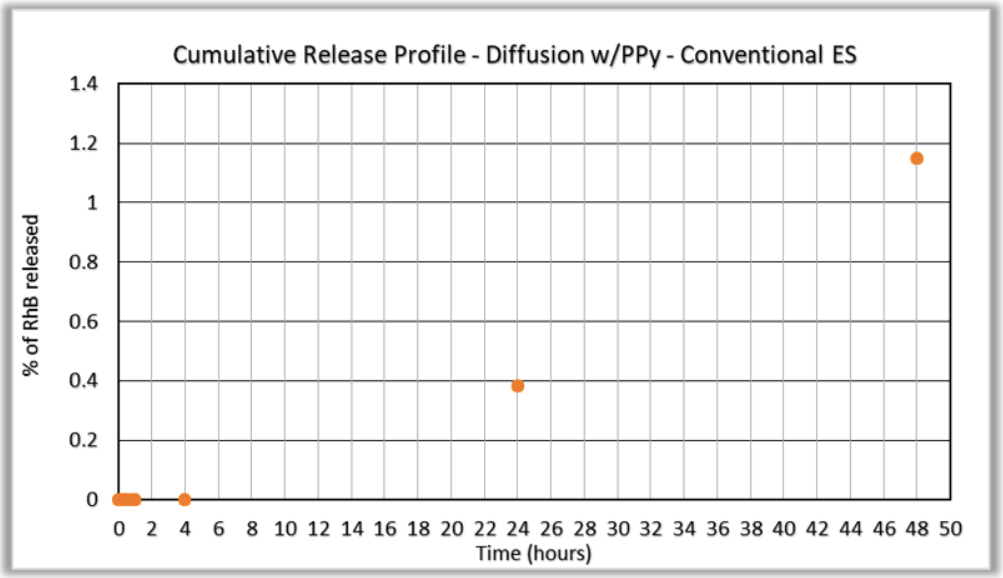

Figure 3.11: Cumulative release profile via diffusion for the case of a conventional coated membrane. Absorbances were measured after 1min, 5min, 10min, 20min, 30min, 50min, 60min, 4h, 24h and 48h membrane had been immersed.

It is important to underline, given the results of the above figures, that despite the measured absorbances had been higher for the conventional electrospun membranes, since the concentration of the model drug encapsulated in these fibers is also higher (7

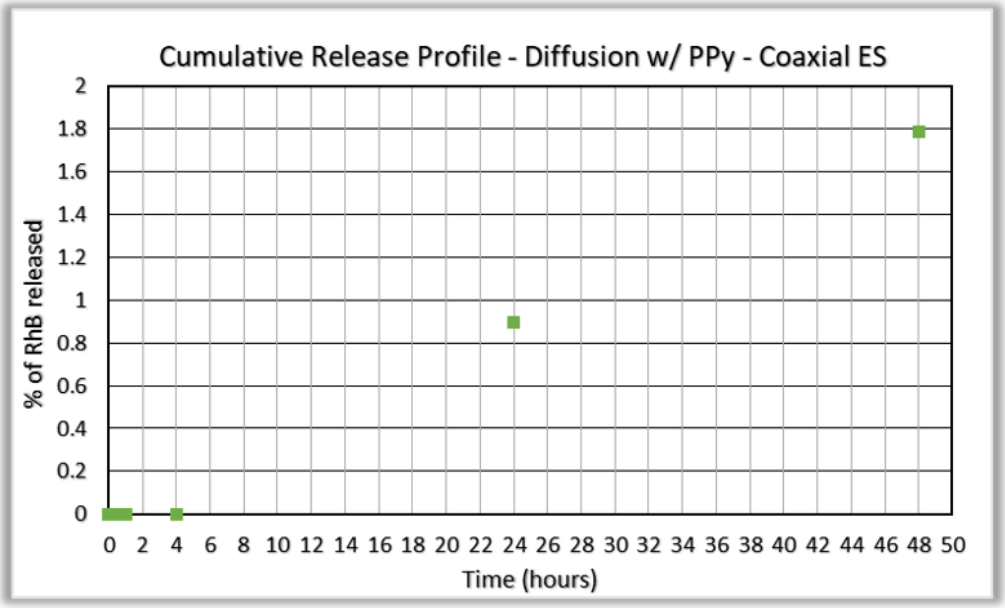

Figure 3.12: Cumulative release profile via diffusion for the case of a coaxial coated membrane. Absorbances were measured after 1min, 5min, 10min, 20min, 30min, 50min, 60min, 4h, 24h and 48h membrane had been immersed.

x 10^{-3} mM) than the one registered for the coaxial case (3 x 10^{-3} mM), when converting it up to percentage, the ratio difference in the equation 3.1 will be much lower for the case of the coaxial membranes, leading to high percentage values. Furthermore, the PPy coating induces significant differences in terms of release profiles. The model drug takes much longer, specially in the conventional electrospun membranes, to diffuse out of the nanofibers and percentages registered are much lower than the ones measured in the uncoated case.

As it can be easily highlighted in the absorbances profiles depicted in Figure 3.7, RhB presents two distinguishable absorbance peaks. Typically, research works that rely on RhB to model a drug in their controlled release studies [31], [32], [54], focus their attention on the absorbances registered for the wavelength of 554 nm, as it is considered the maximal absorbance peak of this substance – as indicated in the Materials Chapter. This also justifies why the calibration curve (Figure 3.8) was calculated for the absorbances measured at the wavelength of 554 nm.

Without any literature support, once again an exploratory study was employed in order to understand what type of results would be obtained depending on the different conditions applied. Table 3.4 lists the different case studies that were outlined and performed. In every case listed, the process was identical, despite the differences between parameters of each case: membrane was partially immersed in a 20 mL volume of water, application of the stimulus was done immediately and, after the corresponding application time, membrane was removed and 3 mL of the solution were measured in the UV-spectrometer.

Table 3.4: List of conditions attempted in electrically controlled drug release studies.

Cases	Polarity	Voltage Used (V)	Time (min)
1	+	0; 1; 2; 5	2
2	-	0; 1; 2; 5	2
3	-	0.5; 0.8; 1; 2	2
4	-	0; 2; 4; 5	5; 10
5	+	0; 2; 5	5; 10; 60
6	+	20	10; 20

Figure 3.13 depicts a representative example of the type of result that was obtained to every case attempted and listed in Table 3.4.

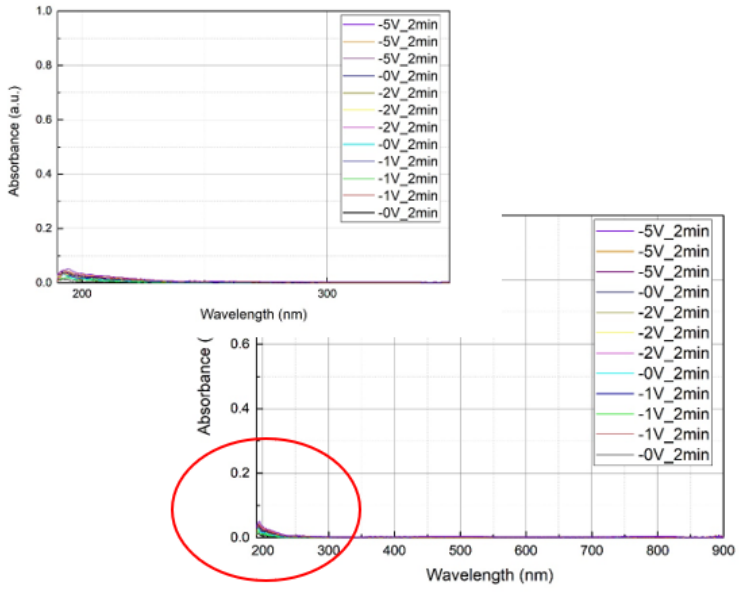

Figure 3.13: Example of curve obtained for case nr. 2 listed in Table 3.4.

From the analysis of the above figure, it can be stated that no reaction, in terms of absorbance variance, was denoted in the region of interest (around 554 nm). Only around the 190 – 200 nm region was that variance registered. However, with a closer look over this area and performing a more quantitative analysis, it is verified that there is no relationship between these values and the change of conditions being applied to the system. Therefore, drug release was not verified for any of the cases mentioned above.

Given the difficulties in obtaining the desired results, a review of the literature was made with the aim of identifying a list of possibilities that could be limiting the diffusion of RhB out of the membrane through application of a stimulus.

Research studies were found on the degradation of RhB, either by temperature or due to UV exposure; it was also considered the hypothesis of, despite the low percentage of the model drug lost during polymerization, the amount left could not be concentrated enough to produce any impact on the absorbance measurement; the ultimate reason pondered to be causing such difficulties was the short period of time that separated the stimulus being applied from the UV-abs measurement.

In order to study the influence of the UV radiation on the samples used in this work, a 2 x 3 cm piece of membrane, produced by the conventional electrospinning technique, was exposed to an UV-light (380 nm) for 3 consecutive hours. After this time, the membrane was immersed in a 20 mL water volume and its diffusion profile was studied and matched with the one previously obtained for the same type of membrane, as represented in figure 3.9.

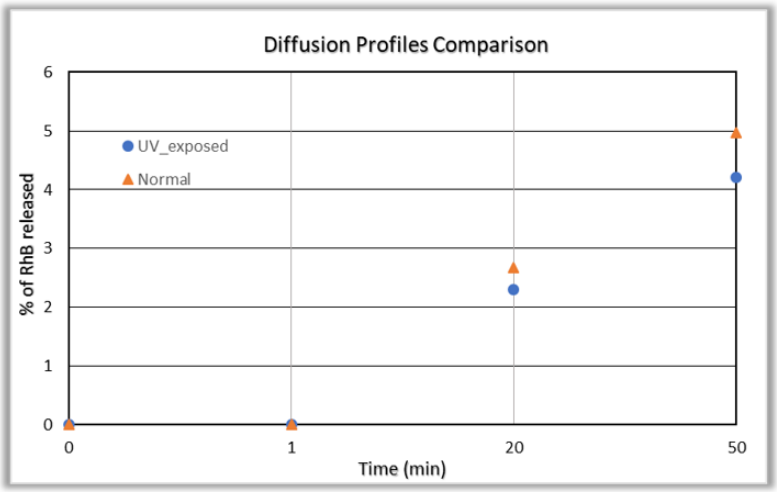

Figure 3.14: Diffusion drug release profiles comparison - UV vs Normal.

From Figure 3.14, it is assumed that UV influence on the membranes used throughout this work can be neglected, due to similarity between values of both profiles. Despite not being in direct contact with any temperature source, any excessive stirring of solutions or any proximity from a temperature source itself in a lab environment could lead to a raise in temperature values at the membranes surface. Thereby, an identical study as

the one discussed above to the UV radiation was performed, for the case of the temperature. According to González and Frey [31], in their research work, they have cured their electrospun membranes containing RhB at a temperature of 180ºC to avoid model drug degradation. The main differences were verified visually, with the reduction of the pink intensive colour, since in terms of drug release, the corresponding profile did not change abruptly, when compared to the normal diffusion one (Figure 3.15).

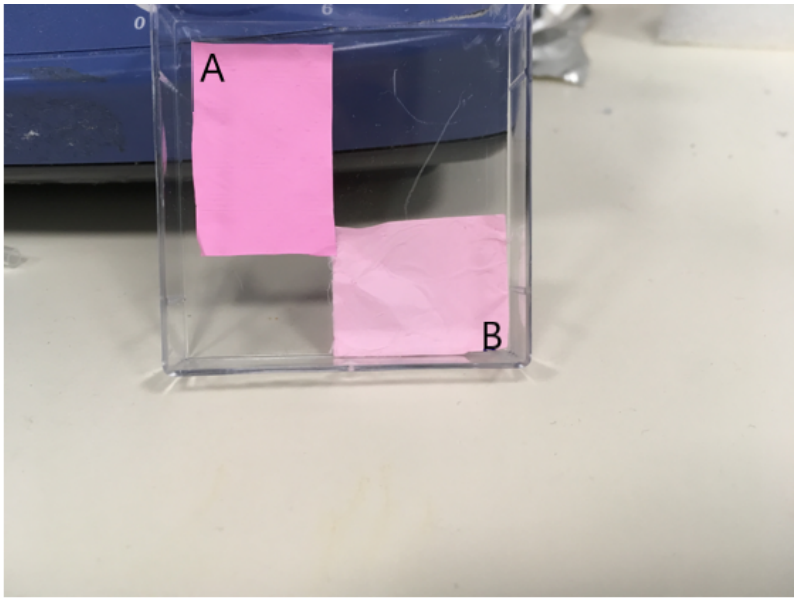

Figure 3.15: Visual difference before (A) and after (B) membrane curing.

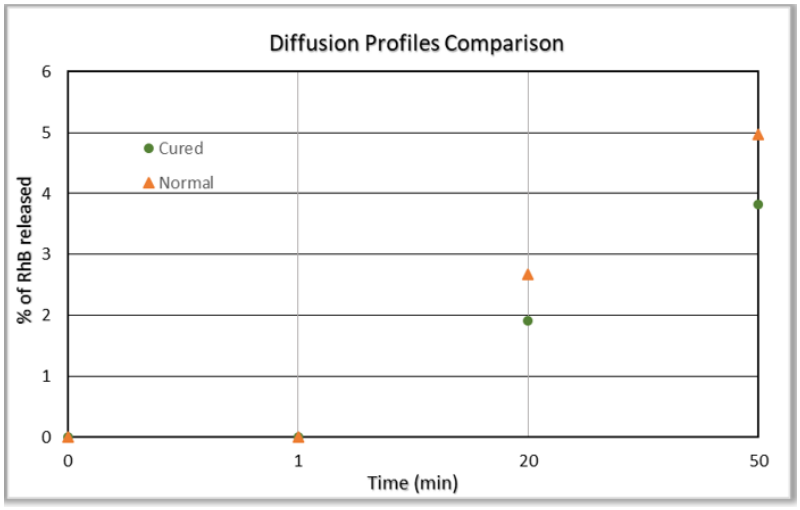

Figure 3.16: Diffusion drug release profiles comparison - Normal vs Cured.

With the aim of identifying if the amount of RhB encapsulated in the membrane was concentrated enough to produce any impact on the absorbance measurement, the membranes that were previously subject to the various stimulus applied in the different case scenarios listed in Table 3.4, were left immersed for a few days and the corresponding

UV-abs values were measured after this period. Figure 3.17 represents an example of the UV-vis absorbance profile of a conventional membrane, previously stimulated with a positive polarity signal, left immersed for 3 days.

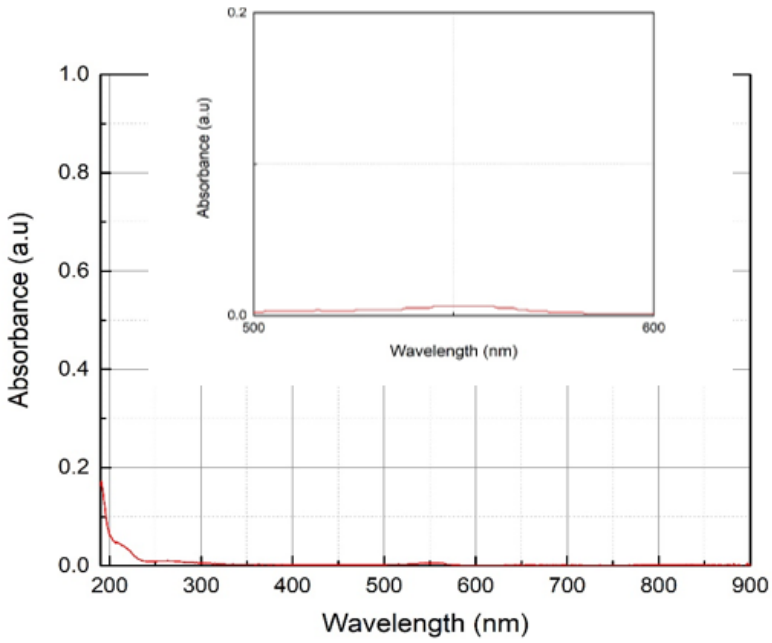

Figure 3.17: UV-vis absorbance profile of a previously stimulated conventional membrane left immersed for 3 days.

It is clearly detectable the short but distinguishable peak in the region of interest, which automatically set aside the hypothesis that was being tested. It turns out that the amount of RhB encapsulated is still enough to be detected by the equipment. This was the onset that led to the final hypothesis thought to be avoiding the release of the model drug under application of an electrical stimulus.

Overviewing the results already discussed: temperature and UV radiation were clarified to not having a relevant impact on the RhB release; it was proven that, by applying stimulus on a membrane and left her immersed for a few days, produced better results than the ones obtained in the moment of performing the tests. That being the case, the procedure adopted to perform the electrically controlled release was modified: instead of applying the stimulus and measuring the absorbance of the medium right after the stimuli application time, it was studied the hypothesis of applying a stimulus and measuring the corresponding absorbances only after a while, specifically 30 minutes. The new method was performed first on membranes produced by conventional electrospinning. In order to compare the resultant profile with the corresponding diffusion one presented in Figure 3.11, a +5V stimuli was applied and then the first absorbance measure was performed only after half an hour, being the last one taken 48h after the stimuli application. Results were repeated for the negative polarity of the signal and then faced against the normal diffusion profile and are represented in Figure 3.18.

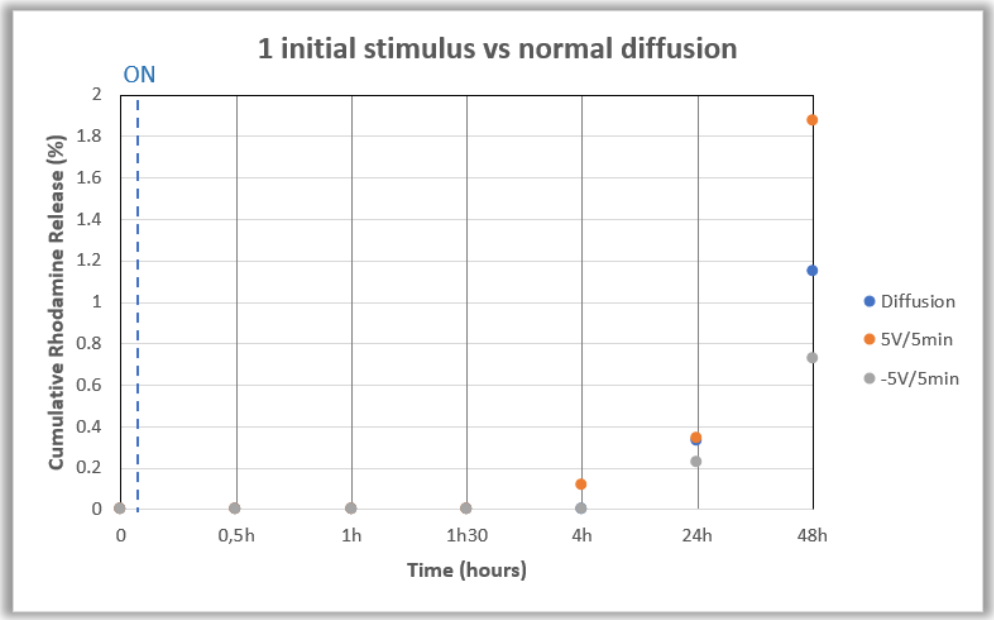

Figure 3.18: Electrically controlled release profiles after 1 single stimulus against normal diffusion release comparison – conventional electrospun membranes.

Interestingly, and despite the low percentages measured during the considered period of time, it is possible to distinguish different behaviors between profiles. It can be stated that, until a certain time, namely 1h30 after stimuli application, any of the profiles presented signals of RhB release. This common scenario is disrupted hours later (4h), moment at which membrane stimulated with the positive polarity signal loses some of the model drug from its nanofibers mat, considerably sooner that the other assessed situations. After 24h, every membrane has already registered a certain absorbance value, being important to highlight that the positive polarity stimuli still present the major response, followed by the membrane subject to normal diffusion and lastly by the other stimulated membrane. Such tendency is reinforced at the measurement performed after 48h, where differences between both stimulated situations is abruptly higher than the previous instant. There are a few conclusions to be withdrawn from this novel approach study: the first being the statement that there is a difference between measuring absorbances right after stimuli application versus this later situation, where membrane is left immersed during a certain period, so that the drug can have time to disassociate from the encapsulating fibers and disseminate to the surrounding medium. Another important conclusion is the difference between polarities of the stimuli. Clearly the positive stimuli induced a much stronger response on the membrane comparing to the opposite polarity. This result was theoretically expected: since the PPy layer is being charged with a positive external stimulus and given the positively charged aminoxanthene group of RhB backbone chain [55], they would repel each other, easing RhB release to the medium. Oppositely, if a negative electronic charge is induced to the conductive polymer, the tendency would be

for the PPy to stronger retain RhB inside the fibers, given their electronic attraction.

Once verified that the positive stimulus was the one to which membranes were more sensitive, impact of the amount of voltage induced was studied. Since the macro objective of developing this kind of systems is to incorporate them into biodevices, as an example, smart wound dressings, voltages over 5V would not be advisable, given the inherent risk it brings to the human wellbeing. Therefore, values below this one were tested, namely +1V and +3V. Additionally to the study of the impact of varying voltage value, this last study was also outlined with the aim of reaching, if possible, the characteristic profile of an on-off switch release system. This switch-like profile would enable an higher control over the drug release, not only in terms of amount released, but also in which instants the release would occur. Ideally, according to the mentioned profile, the membrane would only release the drug in the instants after the stimulus have been applied and would remain approximately constant until the following stimulus application.

That being said, the figure that follows contains a series of dashed lines with the word "ON" at the top. This corresponds to the moment the stimulus was applied. As it was done in the prior study, absorbances were only measured at least after 30 minutes from the moment the stimulus stopped being applied and the duration of the stimulus was also 5 minutes. There was, however, some periods during which the membrane was simply immersed, with no external stimuli application. Absorbances were measured during these periods so that the mentioned on-off desired property could be assessed.

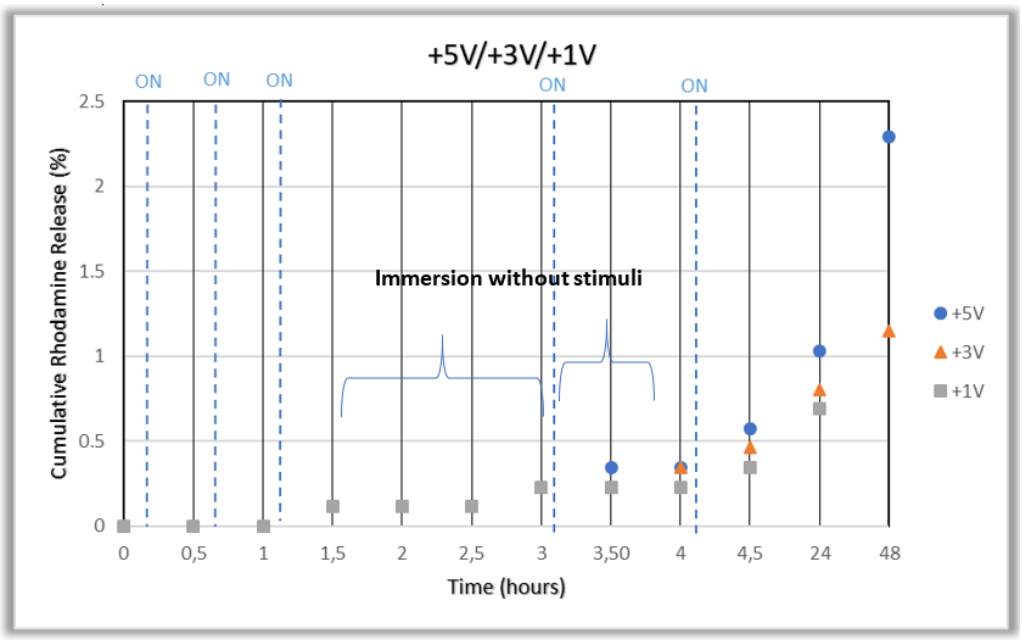

Figure 3.19: Release profiles for different voltage values and "on-off"property study for a conventional electrospinned membrane.

Analyzing Figure 3.19 and comparing it to the previous release profile shown above,

it is important to highlight several common and different aspects between both: as presented in Figure 3.18, in Figure 3.19, despite the extra stimulus applied after half an hour, the percentage of released RhB was still null after one hour of the membranes being immersed. Differences started to be noticed 30 minutes later, where a third applied stimulus led to an earlier RhB release when compared to the scenario studied before. This difference is justified by the application of two additional stimulus in this latter case, leading to the same amount of model drug released for all three voltage values. From this instant of time until the three hours of membrane immersion, no stimulus was applied to the membranes and absorbances continued to be measured in 30-minute intervals. Interestingly, every stimulus applied led to the same result in terms of drug release. The aim of the study during this period was to understand whether the membrane could be considered sensible to a switch on-off profile. Thereby, by maintaining its value of RhB release throughout this period, it meant that no drug was being released without the stimulus application. The exception occurred at the last instant measured (3h), where a subtle rise of the released percentage was registered, probably inherent to some natural diffusion by the amount of time it had been immersed. A new stimulus was applied right after 3h had passed, which it was expected to raise the percentage of drug release, therefore confirming a switch-like profile. However, after 30 minutes, this increase only occurred for the higher voltage applied. The following half an hour had no stimulus application, where it was verified, at the end of this period, that +5V was fitting perfectly in the desired on-off profile; +3V appeared to have a late response to the stimulus applied 1h before and +1V revealed to be less sensitive to the switching stimulus application. A final stimulus was induced after 4h of membrane immersion, where differences between voltage values were emphasized and additional conclusions in terms of release profiles could be withdrawn. At the 4h30 instant, the membrane subject to the +5V voltage confirmed its sensitivity to a switchable on-off profile; followed by the +3V membrane which, despite the slow response to the stimulus, also presented to be sensitive to an on-off system; and the lowest voltage value induced, though the membrane had proven to be sensitive to the stimulus application, with its extremely slow response, it is a system that cannot be characterized by having the capacity to an on-off switchable profile. Later periods assessed, namely 24h and 48h after membrane had been immersed, were useful only to prove that membranes are clearly more sensitive to a higher electrical stimulus, with a significant difference in terms of drug release percentages after two days of immersion.

For the coaxially produced membranes, electrically controlled release studies were extended only until the comparison between the polarity of the stimulus and the normal diffusion release profiles for this type of membranes (equivalent to the results presented in Figure 3.18 in the discussion above). The conditions under which the study was performed were identical to the conventional membranes study, where the stimuli were applied during 5 min and absorbances were measured along the same time intervals, being then converted to release percentages.

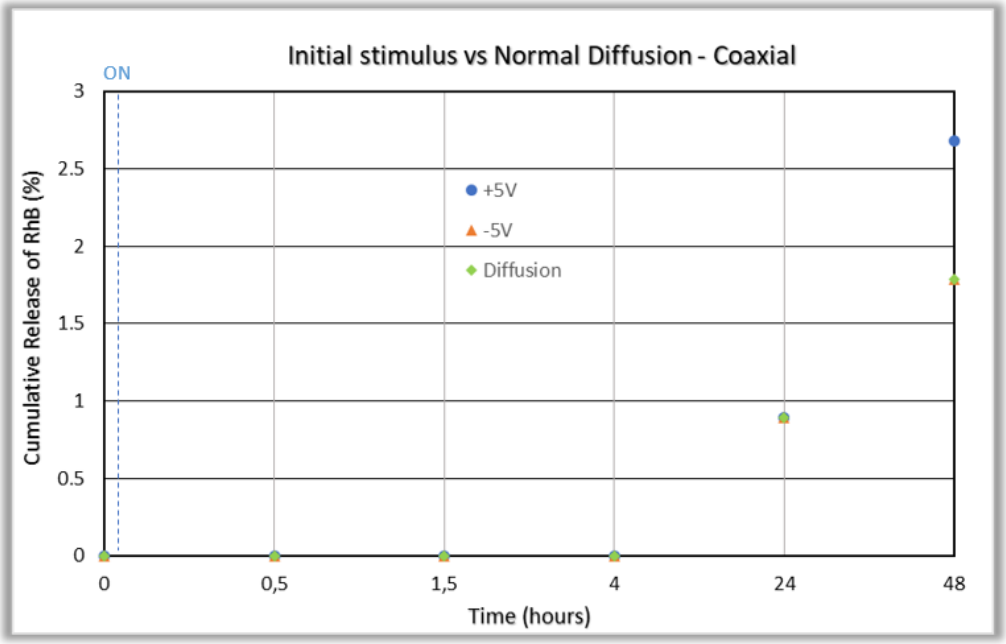

Figure 3.20: Electrically controlled release profiles against normal diffusion release comparison – coaxial electrospun membranes.

Comparing to the conventionally electrospun membranes, differences between voltage values do not induce such significant impact on the membranes release capacity when faced against the profile obtained for the normal diffusion of these membranes in an aqueous solution. However, after 48h of the membrane being immersed, it is visible the higher sensivity of the membrane to the positive polaritity. Once again, the reason behind this behavior is related with the electromigration of RhB towards the electrode, facilitated by electronic repulsion between equal charged molecules of PPy and the model drug.

Beyond the drug release capacity of both types of membranes produced, a further study was performed to understand the impact that electrically controlled applied stimuli can have on the morphology of the given membranes and also if it changes considerably the conductivities previously measured.

SEM images were acquired for the membranes produced by coaxial electrospinning and subject to a 5V stimulus, one with the positive polarity and the other one with the negative.

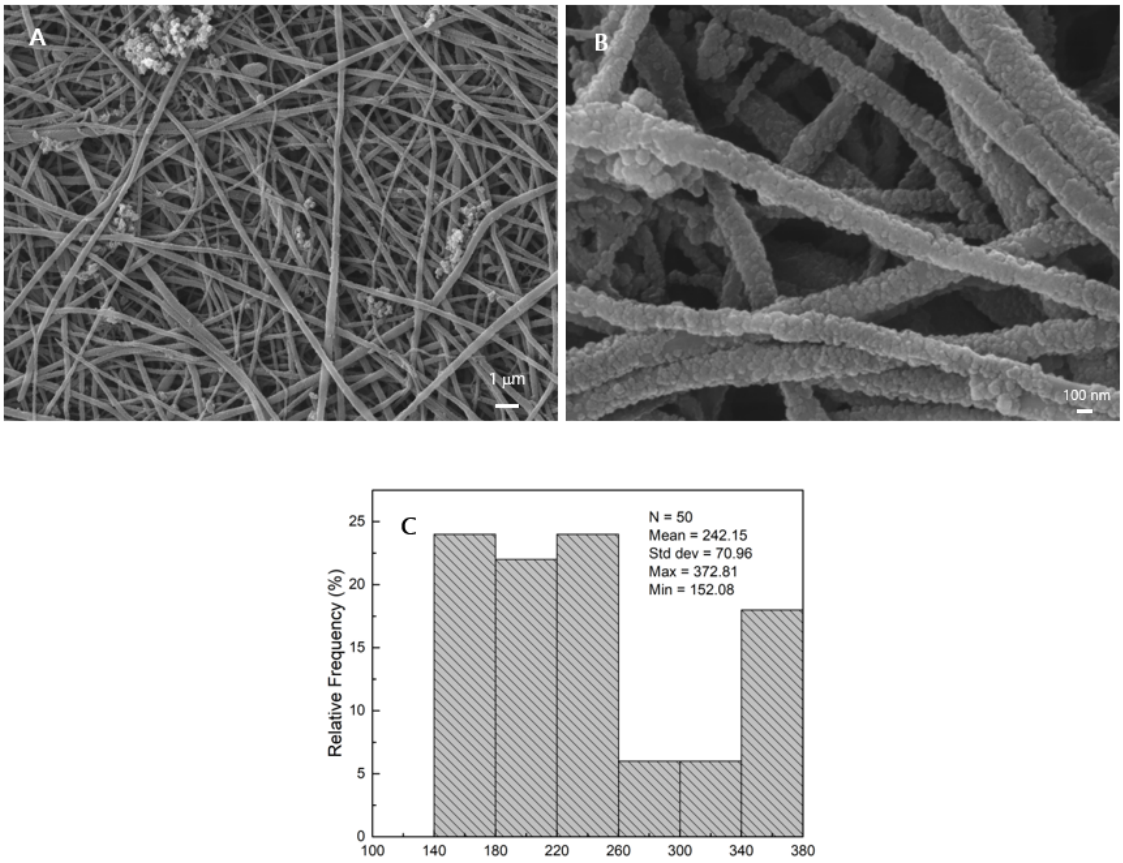

Figure 3.21: SEM images and corresponding histogram for fiber diameter analysis of a coaxial functionalized membrane subject to an external positive stimulus. A corresponds to a magnification of x5000 and B to a magnification of x30000.

The major difference relatively to the membranes case discussed prior to the controlled release tests is the softness of the surface. Whereas on the absence of stimulus, the surface of the analyzed samples looks smoother, after being subjected to the stimulus it gets visually rougher. This change in the surface roughness might be explained by the immersion of a piece of the membrane in the water, so to initiate the tests, period during which some poorly adhered PPy particles may start to disaggregate from the nanofibers. Another possible reason for this morphological change may be due to some conformational changes that might occur when PPy is charged with either positive or negative charges, related to the change of the overall net charge of the polymer [52]. The step of immersing a part of the membrane in the water also explains the reason why nanofibers subjected to the stimulus present larger diameters than those that had just been polymerized (Figures 3.21C and 3.22C). This is due to the swelling behavior that nanofibers are subject to as soon as they start to absorb water, inherently increasing their diameter size [9].

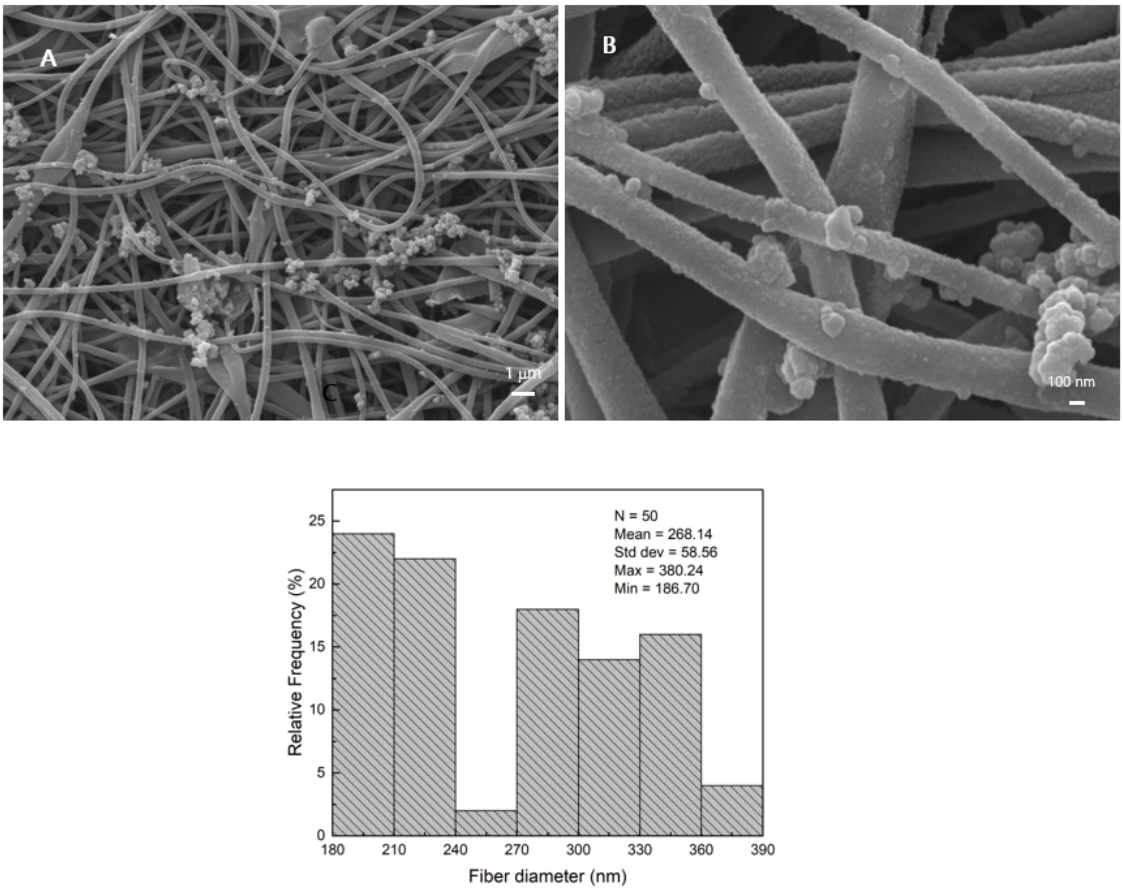

Figure 3.22: SEM images and corresponding histogram for fiber diameter analysis of a coaxial functionalized membrane subject to an external negative stimulus. A corresponds to a magnification of x5000 and B to a magnification of x30000.

Conductivity measurements were performed for the membranes produced by both methods and subject to the studies mentioned above. Comparison between the number of stimuli applied to the membrane is presented and the value chosen was the +5V since it registered the best results during the study. Parameters listed in the Materials and Methods chapter were defined, conductivities were measured and then compared to the values obtained for the coated membranes before controlled release tests (corresponding to the case of 0 number of stimuli applied). Results are summarized in Table 3.5 and discussed below.

Table 3.5: Summary of the conductivities obtained under several conditions studied throughout the work.

Nr stimuli	Voltage	ES-conventional/PPy		ES-coaxial/PPy	
		Planar	Transverse	Planar	Transverse
0		$(6.03\pm0.03)\times10^{-02}$	$(2.84\pm0.05)\times10^{-05}$	$(4.81\pm1.24)\times10^{-02}$	$(2.27\pm1.0)\times10^{-05}$
1	+5V	$(6.96\pm2.14)\times10^{-06}$	$(2.70\pm1.06)\times10^{-08}$	$(9.58\pm2.90)\times10^{-05}$	$(5.43\pm2.27)\times10^{-08}$
	-5V	$(3.40\pm1.48)\times10^{-06}$	$(3.90\pm0.80)\times10^{-07}$	$(8.34\pm1.71)\times10^{-05}$	$(7.85\pm3.49)\times10^{-08}$
Several	+5V	$(2.38\pm0.75)\times10^{-07}$	$(3.85\pm1.37)\times10^{-09}$		

From the values summarized in the above table, a common conclusion to every situation is the fact that the conductivities measured after stimuli application are lower than the ones measured prior to the controlled release studies. This is mainly due to the time during which PPy was immersed in the water, leading to a change of its protonation state and in turn to a different oxidation state as well. Another possible cause to the decrease of conductivity values was the loss of part of the coating during the time membrane was immersed in the water, especially the aggregates of PPy that were less adhered to the nanofibers surface.

For the study where only one stimuli was applied in order to understand to which polarity was the membrane more sensitive, an interesting statement can be made: the conductivities measured in the case of the membrane stimulated with the +5V voltage, which proved to be the polarity to which membranes were more sensitive, registered lower values than the ones obtained for the -5V voltage. It may be justified by the repulsive force that the conductive polymer felt against the oppositely charged RhB, easing some PPy molecules to disaggregate from the surface, which otherwise would not happen if those molecules were attracted to the model drug (it happens in the case of the negative polarity). Repeating the stimulus application for several times would only contribute to this repulsive phenomenon, thereby leading to the even lower conductivities registered in the last case of several stimuli applied.

Chapter 4

Conclusions and future perspectives

In the work hereby presented, the aim was to combine an innovative set of drug-carrier materials, explore both conventional and coaxial electrospinning techniques in order to obtain a uniform nanofiber membrane, coating it with a conductive polymer and studying its behavior as a controlled drug release system.

The membranes production step demanded an extensive and detailed study, especially in the coaxial setup, so that an optimal combination between the carrier and the drug solutions could be found. For this particular setup, an 8% wt. Cellulose Acetate solution was used to form the shell layer, as a 0.6 mM Rhodamine B solution was injected into the core of the nanofibers. Additionally, conventional electrospinning technique was also studied, with the aim of developing a continuous comparison work between membranes obtained via both types of techniques throughout every part of the work. In the conventional setup, an identical amount of RhB (used in the 0.6 mM solution) was added to an 8% wt. solution of CA in order to obtain a unique solution containing both drug and carrier.

Optical Microscopy and SEM were used to characterize the fibers morphology and, mostly by OM, to analyze if the fibers contained RhB in its interior. The main conclusions to be withdrawn from the OM analysis are that conventional electrospun membranes showed a more homogeneous drug distribution over the fibers matrix, compared to the coaxially obtained membranes, where the drug is supposed to be highly concentrated in the nanofibers core. From the SEM analysis, using the coaxial setup to encapsulate RhB, the electrospun fibers showed a higher average diameter and a rough surface. The larger diameters are due to the larger gauge of the outer needle used for coaxial setup when compared with the conventional one. The surface roughness can probably be explained by the interaction of cellulose acetate molecules in the shell with the water molecules embedded in the core (containing RhB).

In terms of membranes functionalization, the conditions previously optimized by Baptista et al. [27] in their study were replicated and adjusted to the work here developed. The 30-minute reaction time stated in the mentioned study proven to be short to fully polymerize the fibers used in the current work. Instead, a 45-minute reaction under constant stirring was applied, inducing a complete functionalization of the whole membranes.

Electrical conductivity values were measured in both configurations (transverse and planar) and were obtained through the corresponding I-V curves. In the planar setup, conductivities are measured between two electrical contacts that are placed in the same plane (membrane´s surface), whereas transverse setup implies that conductivity is measured across the transverse plane (thickness direction) of the membrane. During Py polymerization, the fibers at the surface of membrane are uniformly coated with PPy which contributes to the higher conductivity ($\sim 10^{-2}$ S/cm) obtained using the planar configuration. In transverse configuration, fewer contact points between fibers coated with PPy or an incomplete Py polymerization of the inner fibers of the membranes can explain the difference observed on conductivity values ($\sim 10^{-5}$ S/cm).

After the performance of different studies to analyse the amount of RhB that was loss by passive diffusion (only by immersing the membrane in water), the membranes were exposed to different signal polarities stimuli in order to find out to which polarity were the membranes more sensible, in terms of drug release. As it can be stated by the results presented in the Results and Discussion chapter, the positive stimuli induced a stronger response on the membrane compared to the opposite polarity. Following this conclusion, further studies were carried out to understand the influence that stimuli voltage values could have on the drug release, being at the same time explored the sensibility of the membranes studied to a on-off switchable pattern. The results obtained shown that the higher the voltage value, the better the membrane could follow the desired on-off profile, also releasing higher amounts of RhB. Thereby, by successfully adjusting the system into a switchable-like profile, a better control over the drug release pattern can be obtained.

The main goal of developing this kind of systems is to further integrate them into bioactuators devices, such as a smart wound dressing as an example. Therefore, to achieve something so sensible and efficient as a system like that would require, a lot of work is still to be done. This work, along with several others already developed, aims to contribute to the diversification of functionalities this type of systems can have. Here, it was presented a novel approach to an innovative drug-carrier system, where the capacity of switching the drug release in an on-off pattern-like was tested out. Moreover, the option for organic and biocompatible polymers was made, following a sustainable policy. The choice of a model drug instead of a real one, which for the matter of the studies here performed was justified, also helped and contributed to a reduced overall economic investment, along with the techniques and other materials used.

Despite the difficulties encountered throughout the work, a new idea of future study or application ended up being discovered. Oppositely to the majority of drug delivery

systems, the PPy association to the CA-RhB system clearly hindered the spontaneous release of the model drug from the nanofibers mat, which is typically one of the most common issues associated with these systems. However, the most negative aspect about the results obtained in this work was, in fact, the low percentages of the model drug released. In a future research work working with this same combination, it would be important to study the relationship between RhB and PPy, to better understand how they interact and if that could be a possible cause to the low percentages registered. Having this situation solved, it would certainly need further testing, but it would be an interesting system to be tried out with a real drug and to ponder its integration on a real sensory device.

Bibliography

[1] E. Gianino, C. Miller, and J. Gilmore. "Smart Wound Dressings for Diabetic Chronic Wounds." In: *Bioengineering* 5 (June 2018), p. 51. DOI: 10.3390/bioengineering5030051.

[2] S. Bharambe, A. Darekar, and R. Saudagar. "Wound healing dressings and drug delivery systems: A review." In: *International Journal of Pharmacy and Technology* 5 (July 2013), pp. 2764–2786.

[3] J. K. Patra, Das, L. Fraceto, E. Campos, M. D. P. Rodríguez-Torres, L. Acosta-Torres, L. Diaz-Torres, R. Grillo, M. Swamy, S. Sharma, S. Habtemariam, and H. Shin. "Nano based drug delivery systems: recent developments and future prospects." In: *Journal of Nanobiotechnology* 16 (Dec. 2018). DOI: 10.1186/s12951-018-0392-8.

[4] S. Saghazadeh, C. Rinoldi, M. Schot, S. Saheb Kashaf, F. Sharifi, E. Jalilian, K. Nuutila, G. Giatsidis, P. Mostafalu, H. Derakhshandeh, K. Yue, W. Swieszkowski, A. Memic, A. Tamayol, and A. Khademhosseini. "Drug delivery systems and materials for wound healing applications." In: *Advanced Drug Delivery Reviews* 127 (Apr. 2018). DOI: 10.1016/j.addr.2018.04.008.

[5] H. Derakhshandeh, S. Saheb Kashaf, F. Aghabaglou, I. Ghanavati, and A. Tamayol. "Smart Bandages: The Future of Wound Care." In: *Trends in Biotechnology* 36 (Sept. 2018). DOI: 10.1016/j.tibtech.2018.07.007.

[6] S. Chen, R. Li, X. Li, and J. Xie. "Electrospinning: An enabling nanotechnology platform for drug delivery and regenerative medicine." In: *Advanced Drug Delivery Reviews* 132 (May 2018). DOI: 10.1016/j.addr.2018.05.001.

[7] R. Di Gesù, A. Merlettini, C. Gualandi, and M. Focarete. "Advances in multidrug delivery from electrospun nanomaterials." In: July 2018, pp. 405–430. ISBN: 9780081021989. DOI: 10.1016/B978-0-08-102198-9.00014-4.

[8] S. Tungprapa, I. Jangchud, and P. Supaphol. "Release characteristics of four model drugs from drug-loaded electrospun cellulose acetate fiber mats." In: *Polymer* 48 (Aug. 2007), pp. 5030–5041. DOI: 10.1016/j.polymer.2007.06.061.

[9] O. Suwantong, P. Opanasopit, U. Ruktanonchai, and P. Supaphol. "Electrospun cellulose acetate fiber mats containing curcumin and release characteristic of the herbal substance." In: *Polymer* 48 (Dec. 2007), pp. 7546–7557. DOI: 10.1016/j.polymer.2007.11.019.

[10] V. Pillay, C. Dott, Y. Choonara, C. Tyagi, L. Tomar, P. Kumar, L. Toit, and V. Ndesendo Ph.D. "A Review of the Effect of Processing Variables on the Fabrication of Electrospun Nanofibers for Drug Delivery Applications." In: *Journal of Nanomaterials* 2013 (Jan. 2013). DOI: 10.1155/2013/789289.

[11] F. Anton. "Process and apparatus for preparing artificial threads." Pat. 1975504. 1934. URL: http://www.freepatentsonline.com/1975504.html.

[12] G. Taylor. "Electrically Driven Jets." In: *Proc. R. Soc. Lond. A* (1969), pp. 453–475. DOI: 10.1098/rspa.1969.0205.

[13] X. S. Zong, K. Kim, D. Fang, S. Ran, B. Hsiao, and B. Chu. "Structure and Process Relationship of Electrospun Bioabsorbable Nanofiber Membranes." In: *Polymer* 43 (July 2002), pp. 4403–4412. DOI: 10.1016/S0032-3861(02)00275-6.

[14] P. K. Baumgarten. "Electrostatic spinning of acrylic microfibers." In: *Journal of Colloid and Interface Science* 36.1 (1971), pp. 71–79. ISSN: 0021-9797. DOI: https://doi.org/10.1016/0021-9797(71)90241-4.

[15] G. Kabay, A. Meydan, G. Kaleli Can, C. demirci, and M. Mutlu. "Controlled release of a hydrophilic drug from electrospun amyloid-like protein blend nanofibers." In: *Materials Science and Engineering: C* 81 (Aug. 2017). DOI: 10.1016/j.msec.2017.08.003.

[16] Z. Sun, E. Zussman, A. Yarin, J. Wendorff, and A. Greiner. "Compound Core–Shell Polymer Nanofibers by Co-Electrospinning." In: *Advanced Materials* 15 (Nov. 2003), pp. 1929 –1932. DOI: 10.1002/adma.200305136.

[17] X. Qin. "Coaxial electrospinning of nanofibers." In: Jan. 2017, pp. 41–71. ISBN: 9780081009079. DOI: 10.1016/B978-0-08-100907-9.00003-9.

[18] T.-H. Kao, C.-C. Cheng, C.-F. Huang, and J.-K. Chen. "Using coaxial electrospinning to fabricate core/shell-structured polyacrylonitrile–polybenzoxazine fibers as nonfouling membranes." In: *RSC Adv.* 5 (July 2015), pp. 58760–58771. DOI: 10.1039/C5RA09232A.

[19] Z. Kurban, A. Lovell, S. M. Bennington, D. W. K. Jenkins, K. R. Ryan, M. O. Jones, N. T. Skipper, and W. I. F. David. "A Solution Selection Model for Coaxial Electrospinning and Its Application to Nanostructured Hydrogen Storage Materials." In: 2010.

[20] A. Moghe and B. Gupta. "Co-axial Electrospinning for Nanofiber Structures: Preparation and Applications." In: *Polymer Reviews - POLYM REV* 48 (May 2008), pp. 353–377. DOI: 10.1080/15583720802022257.

[21] T. Nguyen, C. Ghosh, S. Hwang, N. Chanunpanich, and J. Park. "Porous core/sheath composite nanofibers fabricated by coaxial electrospinning as a potential mat for drug release system." In: *International journal of pharmaceutics* 439 (Sept. 2012). DOI: 10.1016/j.ijpharm.2012.09.019.

[22] X. Xia, X. Wang, H. Zhou, X. Niu, L. Xue, X. Zhang, and Q. Wei. "The effects of electrospinning parameters on coaxial Sn/C nanofibers: Morphology and lithium storage performance." In: *Electrochimica Acta* 121 (2014), pp. 345 –351. ISSN: 0013-4686. DOI: https://doi.org/10.1016/j.electacta.2014.01.004.

[23] A. Baptista. "Development of Bio-Batteries based on Electrospun Membranes." Doctoral dissertation. Faculdade de Ciências e Tecnologia - Universidade Nova de Lisboa, 2014.

[24] B. Garner, A. Georgevich, A. J. Hodgson, L. Liu, and G. G. Wallace. "Polypyrrole–heparin composites as stimulus-responsive substrates for endothelial cell growth." In: *Journal of Biomedical Materials Research* 44.2 (1999), pp. 121–129. DOI: 10.1002/(SICI)1097-4636(199902)44:2<121::AID-JBM1>3.0.CO;2-A.

[25] B. Garner, A. Hodgson, G. Wallace, and P. Underwood. "Human endothelial cell attachment to and growth on polypyrrole-heparin is vitronectin dependent." In: *Journal of materials science. Materials in medicine* 10 (Feb. 1999), pp. 19–27. DOI: 10.1023/A:1008835925998.

[26] J. Jin, Z. Huang, G. Yin, J. Lin, Q. Li, and D. Han. "Preparation of Polypyrrole-Protein Composite Films and the Electrochemically Controlled Release of Proteins." In: *Journal of Nanoscience and Nanotechnology* 16.3 (2016), pp. 2283–2290. DOI: doi:10.1166/jnn.2016.10921.

[27] A. Baptista, I. Ropio, B. Romba, J. Nobre, C. Henriques, J. Silva, J. Martins, J. Borges, and I. Ferreira. "Cellulose-based Electrospun Fibers Functionalized with Polypyrrole and Polyaniline for Fully Organic Batteries." In: *Journal of Materials Chemistry A* 6 (Jan. 2018), pp. 256–265. DOI: 10.1039/C7TA06457H.

[28] E.-R. Kenawy, G. Bowlin, K. Mansfield, J. Layman, D. Simpson, E. Sanders, and G. Wnek. "Release of tetracycline hydrochloride from electrospun poly(ethylene-co-vinylacetate), poly(lactic acid), and a blend." In: *Journal of controlled release : official journal of the Controlled Release Society* 81 (June 2002), pp. 57–64. DOI: 10.1016/S0168-3659(02)00041-X.

[29] S. Nista, M. d'Ávila, E. Martinez, A. Silva, and L. Innocentini-Mei. "Nanostructured membranes based on cellulose acetate obtained by electrospinning. Part II. Controlled release profile and microbiological behavior." In: *Journal of Applied Polymer Science* 130 (Nov. 2013). DOI: 10.1002/app.39362.

[30] Y. Liao, L. Zhang, Y. Gao, Z. Zhu, and H. Fong. "Preparation, characterization, and encapsulation/release studies of a composite nanofiber mat electrospun from an emulsion containing poly(lactic-co-glycolic acid)." In: *Polymer* 49 (Nov. 2008), pp. 5294–5299. DOI: 10.1016/j.polymer.2008.09.045.

[31] E. Gonzalez and M. Frey. "Synthesis, characterization and electrospinning of poly(vinyl caprolactam-co-hydroxymethyl acrylamide) to create stimuli-responsive nanofibers." In: *Polymer* 108 (Nov. 2016). DOI: 10.1016/j.polymer.2016.11.053.

[32] Y. Su, Q. Su, W. Liu, G. Jin, X. Mo, and S. Ramakrishna. "Dual-Drug Encapsulation and Release from Core-Shell Nanofibers." In: *Journal of biomaterials science. Polymer edition* 23 (Mar. 2011). DOI: 10.1163/092050611X564137.

[33] A. Guiseppi-Elie. "Electroconductive hydrogels: Synthesis, characterization and biomedical applications." In: *Biomaterials* 31 (Apr. 2010), pp. 2701–16. DOI: 10.1016/j.biomaterials.2009.12.052.

[34] C. Pérez-Martínez, S. Chávez, T. del Castillo-Castro, T. Ceniceros, M. Castillo-Ortega, F. Rodríguez-Félix, and J. Galvez. "Electroconductive nanocomposite hydrogel for pulsatile drug release." In: *Reactive and Functional Polymers* 100 (Dec. 2015). DOI: 10.1016/j.reactfunctpolym.2015.12.017.

[35] W. Li, X. Zeng, H. Wang, Q. Wang, and Y. Yang. "Polyaniline-poly(styrene sulfonate) conducting hydrogels reinforced by supramolecular nanofibers and used as drug carriers with electric-driven release." In: *European Polymer Journal* 66 (Mar. 2015). DOI: 10.1016/j.eurpolymj.2015.03.020.

[36] M. Phiriyawirut and T. Phaechamud. "Gallic Acid-loaded Cellulose Acetate Electrospun Nanofibers: Thermal Properties, Mechanical Properties, and Drug Release Behavior." In: *Open Journal of Polymer Chemistry* 02 (Jan. 2012). DOI: 10.4236/ojpchem.2012.21004.

[37] E. Fortunato, D. Gaspar, I. Cunha, M Mendes, A. Vicente, H. Águas, A. C. Marques, A. Pimentel, D. Nunes, L. C. G. Pereira, and R. Martins. "Paper electronics: a sustainable multifunctional platform." In: *2018 76th Device Research Conference (DRC)* (2018), pp. 1–2.

[38] D. A. Cerqueira. "Caracterização de Acetato de Celulose Obtido a partir do Bagaço de Cana-de-Açúcar por 1 H-RMN H-NMR Characterization of Cellulose Acetate Obtained from Sugarcane Bagasse." In: *Polímeros* 20.2 (2010), pp. 85–91.

[39] A. Taborda. "Development of a Cellulose Acetate Multisensorial." Master's thesis. Faculdade de Ciências e Tecnologia - Universidade Nova de Lisboa, 2017.

[40] I. Ropio. "Biobaterias alimentadas por glucose para aplicações." Master's thesis. Faculdade de Ciências e Tecnologia - Universidade Nova de Lisboa, 2015.

[41] C. Ma. "Highly productive ester crosslinkable composite hollow fiber membranes for aggressive natural gas separations." Doctoral dissertation. Dec. 2012.

[42] G. Liu and H. Lu. "Laser-induced Fluorescence of Rhodamine B in Ethylene Glycol Solution." In: *Procedia Engineering* 102 (Dec. 2015). DOI: 10.1016/j.proeng.2015.01.110.

[43] H. F. Fairbairn. "Thermal Responsive Release of a Model Drug , Rhoadmine B , from Alginate Bead System." In: *Williams Honors College, Honors Research Projects* (2016).

[44] P. Supaphol, O. Suwantong, P. Sangsanoh, S. Srinivasan, R. Jayakumar, and S. V. Nair. "Electrospinning of Biocompatible Polymers and Their Potentials in Biomedical Applications." In: *Biomedical Applications of Polymeric Nanofibers*. Ed. by R. Jayakumar and S. Nair. Springer Berlin Heidelberg, 2012, pp. 213–239. DOI: 10.1007/12_2011_143.

[45] H. Cheng, X. Yang, X. Che, M. Yang, and G. Zhai. "Biomedical application and controlled drug release of electrospun fibrous materials." In: *Materials Science and Engineering: C* 90 (May 2018). DOI: 10.1016/j.msec.2018.05.007.

[46] Pharma-exceptients. *Biomedical Applications of Electrospun Nanofibers: Drug and Nanoparticle Delivery*. URL: https://www.pharmaexcipients.com/speciality-excipient/electrospun-nanofibers-drug-and-nanoparticle-delivery/.

[47] *Coaxial needles for electrospinning*. Linari Engineering. 2010.

[48] H. Kurosu. "Chapter 16 - Electrically-Conducting Polymers." In: *Solid State NMR of Polymers*. Ed. by I. Ando and T. Asakura. Vol. 84. Studies in Physical and Theoretical Chemistry. Elsevier, 1998, pp. 589–611. DOI: https://doi.org/10.1016/S0167-6881(98)80024-4.

[49] L. Romano, A. Camposeo, R. Manco, M. Moffa, and D. Pisignano. "Core-Shell Electrospun Fibers Encapsulating Chromophores or Luminescent Proteins for Microscopically Controlled Molecular Release." In: *Molecular pharmaceutics* 13.3 (2016), 729—736. ISSN: 1543-8384. DOI: 10.1021/acs.molpharmaceut.5b00560.

[50] Y. Wang, B. Wang, W. Qiao, and T. Yin. "A Novel Controlled Release Drug Delivery System for Multiple Drugs Based on Electrospun Nanofibers Containing Nanoparticles." In: *Journal of pharmaceutical sciences* 99 (Dec. 2010), pp. 4805–11. DOI: 10.1002/jps.22189.

[51] S. Sayed Ashfaq Ali, M. Firlak, S. Berrow, N. Halcovitch, S. Baldock, B. Yousafzai, R. Hathout, and J. Hardy. "Electrochemically Enhanced Drug Delivery Using Polypyrrole Films." In: *Materials* 11 (July 2018), p. 1123. DOI: 10.3390/ma11071123.

[52] J. Ge, E. Neofytou, T. Cahill, R. Beygui, and R. Zare. "Drug Release from Electric-Field-Responsive Nanoparticles." In: *ACS nano* 6 (Nov. 2011), pp. 227–33. DOI: 10.1021/nn203430m.

[53] G. Jeon, S. Yang, J. Byun, and J. Kim. "Electrically Actuatable Smart Nanoporous Membrane for Pulsatile Drug Release." In: *Nano letters* 11 (Mar. 2011), pp. 1284–8. DOI: 10.1021/nl104329y.

[54] P. Bartasun, H. Cieśliński, A. Bujacz, A. Wierzbicka-Woś, and J. Kur. "A Study on the Interaction of Rhodamine B with Methylthioadenosine Phosphorylase Protein Sourced from an Antarctic Soil Metagenomic Library." In: *PloS one* 8 (Jan. 2013), e55697. DOI: 10.1371/journal.pone.0055697.

[55] I. Moreno-Villoslada, M. Jofré, V. Miranda, R. Gonzalez, T. Sotelo, S. Hess, and B. Rivas. "pH Dependence of the Interaction between Rhodamine B and the Water-Soluble Poly(sodium 4-styrenesulfonate)." In: *The journal of physical chemistry. B* 110 (July 2006), pp. 11809–12. DOI: 10.1021/jp061457j.